AN ABSTRACT OF THE THESIS OF

Ming-Lei Wang for the degree of Master of Science in Chemical Engineering, presented on May 6, 1999. Title: Dechlorination of 2,4,6-trichlorophenol on Bimetallic Pd/Fe Catalyst in a Magnetically Stabilized Fluidized Bed.

Abstract approved: _____
Goran N. Jovanovic

In this work, we investigated the chemical kinetics of the dechlorination of 2,4,6-trichlorophenol on the Pd/Fe catalyst. Four experiments, dechlorination of 2,4,6-trichlorophenol, 2,4-dichlorophenol, 2,6-dichlorophenol, and p-chlorophenol were run in a batch reactor. All factors that will effect the reaction kinetics including system pH, Pd/Fe interfacial area, and Pd/chlorine removal were controlled at the same conditions.

The pseudo-first order rate with respect to the chlorinated hydrocarbon concentration is found to be the appropriate model.

$$-\frac{d\left(VC_A\right)}{dt} = (kW)C_A a = k^* C_A a \qquad (2.11)$$

$$-\frac{da}{dt} = k_d a^n \qquad (2.12)$$

The possible path way for dechlorinating 2,4,6-trichlorophenol to phenol was proposed.

The rate equation for all compounds in this reaction were then developed as follows:

$$-\frac{d\left(VC_1\right)}{dt} = (k_1^* + k_2^*)C_1 a \qquad (2.13)$$

$$-\frac{d(VC_2)}{dt} = (k_3^* + k_4^*)C_2 a - k_1^* C_1 a \tag{2.14}$$

$$-\frac{d(VC_3)}{dt} = k_5^* C_3 a - k_2^* C_1 a \tag{2.15}$$

$$-\frac{d(VC_4)}{dt} = k_6^* C_4 a - k_3^* C_2 a \tag{2.16}$$

$$-\frac{d(VC_5)}{dt} = k_7^* C_5 a - k_4^* C_2 a - k_5^* C_3 a \tag{2.17}$$

$$-\frac{d(VC_6)}{dt} = -k_6^* C_4 a - k_7^* C_5 a \tag{2.18}$$

These rate equations were solved numerically and coupled with all the experimental data to determine the reaction rate constants and deactivation rate constant.

The other object of this work was to investigate the mass transfer phenomena in the application of the Pd/Fe catalyst for remediation of contaminated liquid in Magnetically Stabilized Fluidized Bed. Two experiments were made in the Magnetically Stabilized Fluidized Bed. The mathematical model for this reactor system was developed and was solved by using finite difference method. Four parameters, reaction rate constant k, deactivation rate constant k_d, diffusion coefficient De, and mass transfer coefficient k_l were determined through an optimization procedure.

Dechlorination of 2,4,6-trichlorophenol on Bimetallic Pd/Fe Catalyst in a Magnetically Stabilized Fluidized Bed.

by

Ming-Lei Wang

A Thesis Submitted
to
Oregon State University

In Partial Fulfillment of
the requirements for the
degree of

Master of Science

Presented May 6, 1999
Commencement June, 1999

Master of Science thesis of Ming-Lei Wang presented May 6, 1999

Approved:

Major Professor, representing Chemical Engineering

Head of Department of Chemical Engineering

Dean of Graduate School

I understand that my thesis will become part of the permanent collection of Oregon State University libraries. My signature below authorizes release of my thesis to any reader upon request.

Redacted for privacy

Ming-Lei Wang, Author

Table of Contents

Table of Contents, Continued

Table of Contents, Continued

List of Figures

List of Figures, Continued

List of Figures, Continued

List of Figures, Continued

List of Tables

List of Appendices

List of Appendix Figures

Nomenclature

A_{bd}	Total area in differential "slice" in alginate bead, m2 bead
A_{gl}	Gel liquid area in differential "slice" of bead
A'	External bead surface area/unit bulk liquid volume, m^2/m^3
a	Catalyst activity [-]
C_1	Concentration of 2,4,6-trichlorophenol, mol/m^3
C_2	Concentration of 2,4-dichlorophenol, mol/m^3
C_3	Concentration of 2,6-dichlorophenol, mol/m^3
C_4	Concentration of *p*-chlorophenol, mol/m^3
C_5	Concentration of *o*-chlorophenol, mol/m^3
C_6	Concentration of phenol, mol/m^3
C_A	Concentration of compound A, mol/m^3
$C_{A,0}$	Initial concentration of compound A , mol/m^3
C_b	Bulk concentration, mol/m^3
$C_{b,0}$	Initial bulk concentration, mol/m^3
C_l	Alginate bead liquid concentration, mol/m^3
C_H	Concentration of H^+ in solution, mol/m^3
C_{H^*}	Concentration of H^* in solution (reactive intermediate), mol/m^3
D_{AB}	Diffusivity of a solute, A, in water, B, m^2/s
D_e	Diffusion coefficient for 2,4,6-trichlorophenol in alginate beads, m^2/s
d_b	Diameter of alginate bead, m
F	Sample extration rate, m^3/s

Nomenclature, Continued

F_b	Bouyancy force exerted on the particle, N
F_d	Drag force exerted on the particle, N
F_g	Gravitational force exerted on the particle, N
[H+]	Concentration of hydrogen ions in solution, moles/m^3
H	Magnetic field intensity, A/m
k_l	Liquid-solid mass transfer coefficient in MSFB, m/s
k	Dchlorination reaction rate constant based on amount of catalyst, $m^3/kg_{catalyst}$ s
k*	Dchlorination reaction rate constant coupled with amount of catalyst, m^3/s
k_1*	Rreaction rate coefficient for dechlorinating 2,4,6TCP to 2,4DCP, m^3/s
k_2*	Rreaction rate coefficient for dechlorinating 2,4,6TCP to 2,6DCP, m^3/s
k_3*	Rreaction rate coefficient for dechlorinating 2,4TCP to p-CP, m^3/s
k_4*	Rreaction rate coefficient for dechlorinating 2,4TCP to o-CP, m^3/s
k_5*	Rreaction rate coefficient for dechlorinating 2 ,6TCP to o-CP, m^3/s
k_6*	Rreaction rate coefficient for dechlorinating p-CP to phenol, m^3/s
k_7*	Rreaction rate coefficient for dechlorinating o-CP to phenol, m^3/s
k_d	Deactivation rate coefficient for H_2 (g) passivation, 1/s
m	($\Delta\bullet$ /ΔH); Change of bed voidage with magnetic field intensity, m/A
n	Deactivation order
r	Bead radius, mm

Nomenclature, Continued

Re	Reynolds number, [-]
Sc	Schmidt number, [-]
Sh	Sherwood number, [-]
t	Time, s
u_o	Liquid superficial velocity, m/s
u_{int}	Liquid interstitial velocity, m/s
V	Volume of reactor liquid, m^3
V_0	Initial volume of reactor liquid, m^3
V_{bd}	Volume of alginate bead, m^3
V'_{bd}	Total volume of alginate bead in reactor, m^3
V_{gl}	Volume of free liquid in bead, m^3
W	Weight of catalyst Pd, g
x_{wt}	Mass fraction of ferromagnetic powder in beads, [-]

Nomenclature, Continued

Greek symbols

ε	Reactor voidage in magnetically stabilized fluidized bed (H≠0), [-]
ε_o	Reactor voidage in conventional fluidized bed (H=0), [-]
ε_m	Average bed voidage in the stabilized regime, [-]
ε_p	Average bed voidage in the random motion regime, [-]
μ_l	Liquid viscosity, Pa-s
ν_l	Liquid kinematic viscosity, m^2/s
ρ_l	Liquid density, kg/m^3
ϕ	Fraction of gel solid within the alginate bead

Dechlorination of 2,4,6-trichlorophenol on Bimetallic Pd/Fe Catalyst in a Magnetically Stabilized Fluidized Bed

CHAPTER 1

INTRODUCTION

Chlorinated phenols are commonly used in industry mainly as biocides, insecticides, herbicides, and wood preservatives. They have been detected in water, soil, and air (Passivirta et. al, 1988; Suntio et. al, 1988) because of the misuse, accidental spillage, and improper disposal. The effect of these compounds on the environment are of great concern because of their toxicity, resistance to degradation, and tendency to accumulate in human tissues. They are included in the U.S. Environmental Protection Agency Priority Pollutant List and are carcinogenic substances (Federal Register 1987).

Several technologies have been proposed for dechlorination of chlorinated hydrocarbons in water and soil including: biodegradation (Liu et. al, 1996), soil vapor extraction (McCann et. al, 1994), and surfactant-enhanced washing (Abdul et. al, 1992). These technologies are not always appropriate solutions to a given pollution problem and very often they have serious shortcomings. The biodegradation technology needs long degradation times for achieving acceptable results. The soil vapor extraction and surfactant-enhanced washing, remove chlorinated hydrocarbon

from soil but generates large quantities of secondary wastes which must be again properly addressed.

Another useful technique which uses Pd/Fe bimetal catalyst for the conversion of chlorinated hydrocarbon into ordinary hydrocarbon has been recently reported (Muftikian et. al, 1995; Grittini et. al, 1995, Graham and Jovanovic, 1998). Several technology studies have reporte excellent results for dechlorination of chlorinated organics, particularly chlorinated phenols (compounds such as p-chlorophenol, pentachlorophenol and PCBs), by using powder Pd/Fe catalyst (Muftikian et. al, 1995; Grittini et. al, 1995, Graham and Jovanovic, 1998). Further, the kinetic of dechlorination of p-chlorophenol on the powder Pd/Fe catalyst was studied in an engineering system, Magnetically Stabilized Fluidized Bed (MSFB) capable of delivering catalytic action under real environmental conditions. (Graham, 1998).

The MSFB is a traditional fluidized bed with the addition of a magnetic field. It is sought as an engineering plateform for delivering catalytic action of the Pd/Fe catalyst. Active substances, such as the Pd/Fe catalyst, are entrapped in fluidized beads which are made of a crosslinked Na-alginate. The advantage of the application of the magnetic field is the enhancement of the mass transfer between the bulk liquid and magnetically susceptible beads while aiding in the retention of beads within the fluidized bed (Al-Mulhim, 1995).

Though the kinetics of the dechlorination of a monochlorophenol (p-chlorophenol) on the Pd/Fe catalyst have been extensively studied (Graham and Jovanovic, 1998), the dechlorination of multichlorinated chlorophenols on this bimetal catalyst have not been investigated. In this study, 2,4,6-trichlorophenol is chosen to be dechlorinated by using Pd/Fe catalyst and the kinetics of this serial-parallel dechlorination reaction is explored. The second objective of this work is to confirm the applicability of MSFB technology in the dechlorination of 2,4,6-trichlorophenol contaminated liquid.

Chapter two of this thesis provides the supporting theory for the most appropriate interpretation of the chemical reaction scheme including the proposed mechanism and reaction rate equations. The mathematical model for the reaction and the mass transfer associated with the application of the entrapped Pd/Fe catalyst is also developed and the important characteristics of the MSFB are also incorporated. Chapter three describes the laboratory equipment, materials, and the methods used in the experimental work. Chapter four presents the experimental data and Chapter five interprets these data. The overall disscusion is related to the mathematical model whose parameters are fitted to the experimental data. Chapter six completes this work with conclusion and recommendations. Other details of the experimental method and numerical approximations used in the modeling are provided in the appendices.

CHAPTER 2

BACKGROUND

2.1 Dechlorination Reaction Chemistry

2.1.1 *Reaction Stoichiometry*

Three types of chemical reactions are involved in the dechlorination reaction process on the surface of the Pd/Fe catalyst as reported by Graham and Jovanovic (1998). The first are the various surface reactions. These include the dissolution of iron from the zero-valent state and the consumption of hydrogen ion on both the iron and palladium surfaces as represented by Equation 2.1 to 2.3. The second are solution reactions as described by Equation 2.4 and 2.5. The abundance of hydrogen, H^+, is controlled by its formation from the solution reactions and its removal by Fe to form $H_2(g)$ or Pd to form the intermediate reactive hydrogen, H*. The third type of reaction is the actual reaction of chlorine removal step (Equation 2.6). The actual mechanism of this reaction within reaction system used in this study is not known. Equation 2.6 represents probably several consequential reaction steps. The electrons produced in the iron dissolution reaction are used by the palladium surface to form the highly reactive intermediate, H*, which is used in the dechlorination reaction.

Surface Reactions:

$$Fe^0 \rightarrow Fe^{2+} + 2e^- \qquad (2.1)$$

$$2H^+ + 2e^- \xrightarrow{Fe} H_2\,(g) \qquad (2.2)$$

$$H^+ + e^- \xrightarrow{Pd} H^* \quad (2.3)$$

Solution Reactions:

$$2H_2O \rightarrow 2H^+ + 2OH^- \quad (2.4)$$

$$2HCl \rightarrow 2H^+ + 2Cl^- \quad (2.5)$$

Dechlorination Reaction:

$$2H^* + R\text{-}Cl \rightarrow R\text{-}H + HCl \quad (2.6)$$

Figure 2.1 shows this multi-step reaction process.

Several other reactions can take place simultaneously in the reaction volume. Of particular interest are $Fe^{2+}+2OH^- \rightarrow Fe(OH)_2$ ($pH \geq 6$). Similarly the formation of $Fe(OH)_3$ can take place at even lower pH if oxygen is present in the system.

$Fe(OH)_2$, $Fe(OH)_3$, and hydrogen bubbles (Equation 2.2) are formed on the surface of the catalyst while the dechlorination reaction proceeds. These reaction products cover the Pd/Fe intersurface where the dechlorination reaction takes place. This may result into deactivation of the Pd/Fe catalyst. Figure 2.2 shows this deactivation mechanism. The deactivation mechanism is dependent on the system pH and dissolved O_2, and can be controlled by adjusting pH in a deoxygenated environment (Grahm and Jovanovic, 1998).

2.1.2 *Rate Equation for Dechlorination Chemical Kinetics on Powder Pd/Fe Catalyst*

The rate of dechlorination of chlorinated hydrocarbon (denoted as A) on powder Pd/Fe catalyst is related to the concentration of A and H*, and the amount of catalyst, W, as shown in Equation 2.8. The form of this kinetics equation was found to be adequate for the representation of the dechlorination reaction process by Graham and Jovanovic (1998). The production of H* at the surface of palladium as indicated in the surface reaction was assumed to be constant at constant pH. If pH is maintained at constant value, the concentration of H* can be assumed constant and combined with k' to give k. this can be further combined with the catalyst weight to give an overall rate constant, k*

$$-\frac{1}{W}\frac{d(VC_A)}{dt} = k' \; C_A C_{H^*} \tag{2.8}$$

$$-\frac{d(VC_A)}{dt} = (Wk)C_A = k^* C_A \tag{2.9}$$

Therefore, $k^* = k' W C_{H^*}$ (2.10)

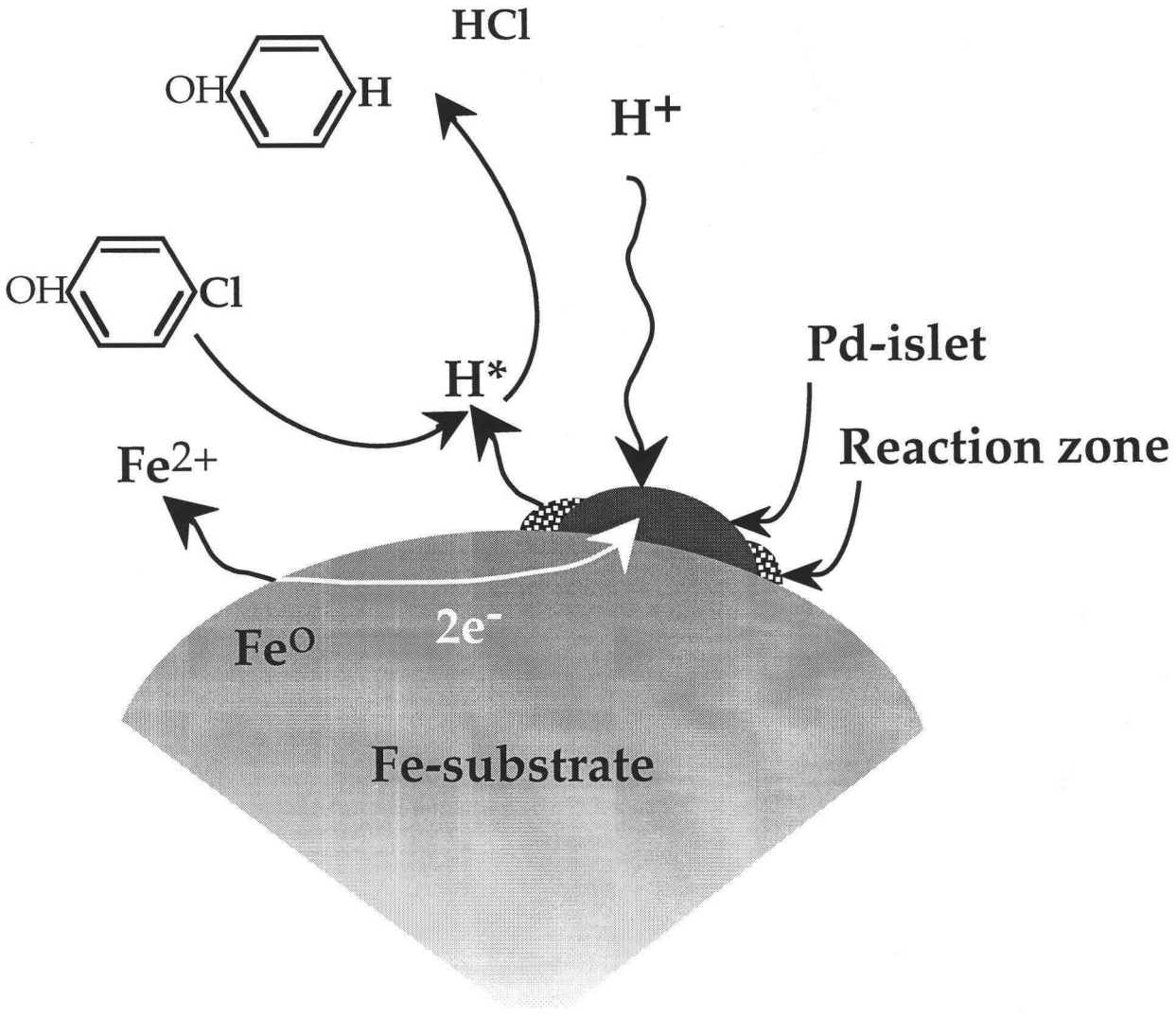

Figure 2.1 Multi-step dechlorination reaction on the Pd/Fe catalyst

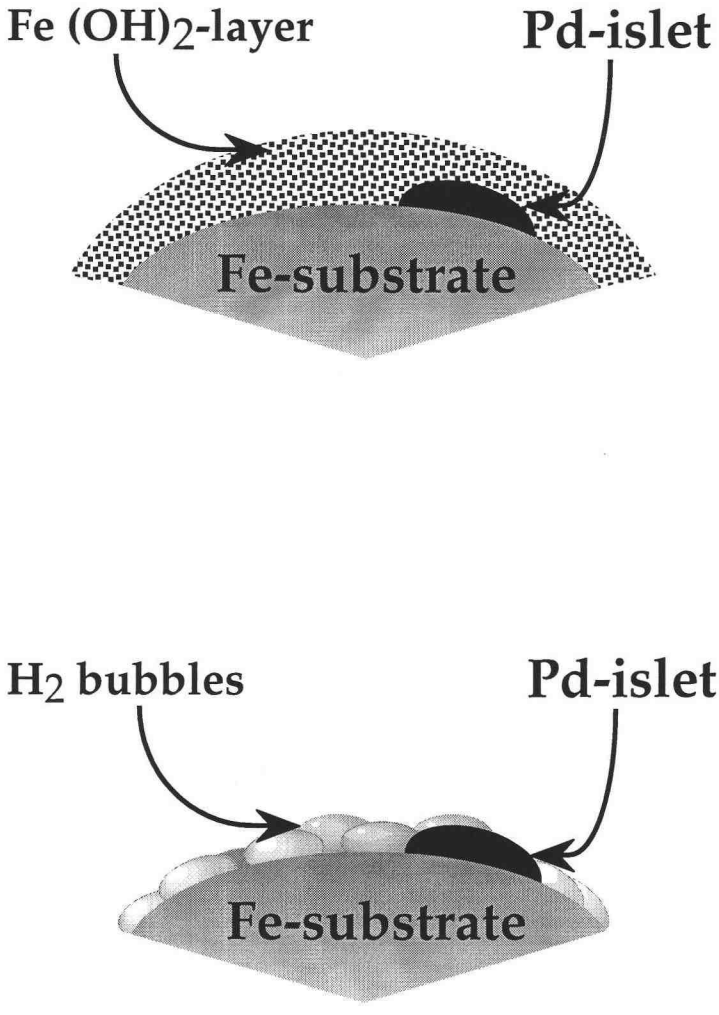

Figure 2.2 $Fe(OH)_2$, $Fe(OH)_3$ and hydrogen bubble formation on the Pd/Fe catalyst surface

As described in section 2.2.1, $Fe(OH)_2$, $Fe(OH)_3$, and hydrogen bubbles form on the surface of Pd/Fe catalyst and may increase the resistance of the overall dechlorination reaction process. An activity term, *a*, thus is added into the rate equation as shown in Equation 2.11 to accommodate for deactivation process. This term describes a decrease in catalyst activity by a loss of dechlorination sites (Levenspiel, 1996). The activity of the Pd/Fe catalyst may be described by the Equation 2.12 as an n^{th} order expression.

$$-\frac{d\left(VC_A\right)}{dt} = (kW)C_A a = k^* C_A a \qquad (2.11)$$

$$-\frac{da}{dt} = k_d a^n \qquad (2.12)$$

However it was found by Graham and Jovanovic (1998) that a value of n=1 suitably represents the deactivation process.

2.1.3 *Determination of Reaction Rate Constants of Dechlorination of 2,4,6-trichlorophenol*

The reaction of dechlorination of 2,4,6-trichlorophenol on powder Pd/Fe catalyst is shown in Figure 2.3 as a multiple step reaction.

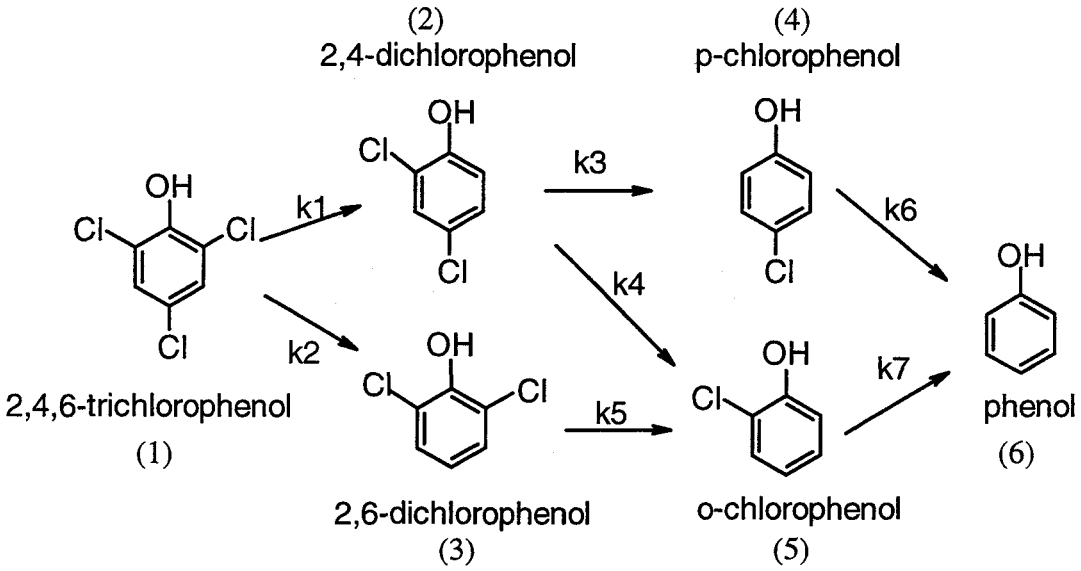

Figure 2.3 Illustration of dechlorination of 2,4,6-trichlorophenol on Pd/Fe catalyst

Phenol is the final product. Intermediates such as 2,4-dichlorophenol, 2,6-dichlorophenol, p-chlorophenol, and o-chlorophenol are formed and are simultaneously dechlorinated by the catalyst. Denote 2,4,6-trichlorophenol, 2,4-dichlorophenol, 2,6-dichlorophenol, p-chlorophenol, o-chlorophenol, and phenol as species 1, 2, 3, 4, 5, and 6 respectively. Dechlorination rate equations of all the compounds in this multiple reaction can be represented with the kinetic form, Equation 2.11. Therefor,

$$-\frac{d(VC_1)}{dt} = (k_1^* + k_2^*)C_1 a \qquad (2.13)$$

$$-\frac{d(VC_2)}{dt} = (k_3^* + k_4^*)C_2 a - k_1^* C_1 a \qquad (2.14)$$

$$-\frac{d(VC_3)}{dt} = k_5^* C_3 a - k_2^* C_4 a \tag{2.15}$$

$$-\frac{d(VC_4)}{dt} = k_6^* C_4 a - k_3^* C_2 a \tag{2.16}$$

$$-\frac{d(VC_5)}{dt} = k_7^* C_5 a - k_4^* C_2 a - k_5^* C_3 a \tag{2.17}$$

$$-\frac{d(VC_6)}{dt} = -k_6^* C_4 a - k_7^* C_5 a \tag{2.18}$$

initial condition for these differential equations are:

at $t=0$,

$$C_1 = C_{1,0} \tag{2.19}$$

$$C_2 = C_3 = C_4 = C_5 = C_6 = 0 \tag{2.20}$$

2.2 Modeling Dechlorination of 2,4,6-trichlorophenol in Alginate Beads With Entrapped Pd/Fe Catalyst

Figure 2.4 schematically represents the MSFB dechlorination reactor system. The chlorinated organic is first convectively transported to the surface of the bead and then it diffuses into the gel beads. The dechlorination reaction and deactivation of catalyst take place inside the beads. The assumptions for this system are made as

follow:

1. The Pd/Fe catalyst is entrapped within the gel beads and not permitted into the bulk liquid.
2. The alginate gel beads are of equal size and are uniform spheres of radius, R.
3. A constant effective diffusion coefficient, D_e, exists throughout the gel beads. Hence, the tortuosity effect on the aqueous diffusion coefficient is not changing from the surface of the alginate bead to the center. This assumption implies that alginate gel beads are homogeneously polymerized or cross-linked.
4. No reaction is occurring in the bulk of the liquid.
5. The Pd/Fe catalyst is homogeneously entrapped within the gel bead thus ensuring a uniform reaction surface throughout the gel bead.
6. The gel bead liquid is defined as a volume fraction of the total bead volume. The symbol, ϕ, represents the fraction of bead occupied by gel and/or entrapped substance.
7. The gel bead open area for diffusion is defined as a fraction, $1-\phi$, of the total surface area and is dependent upon the fraction of bead surface occupied by gel.

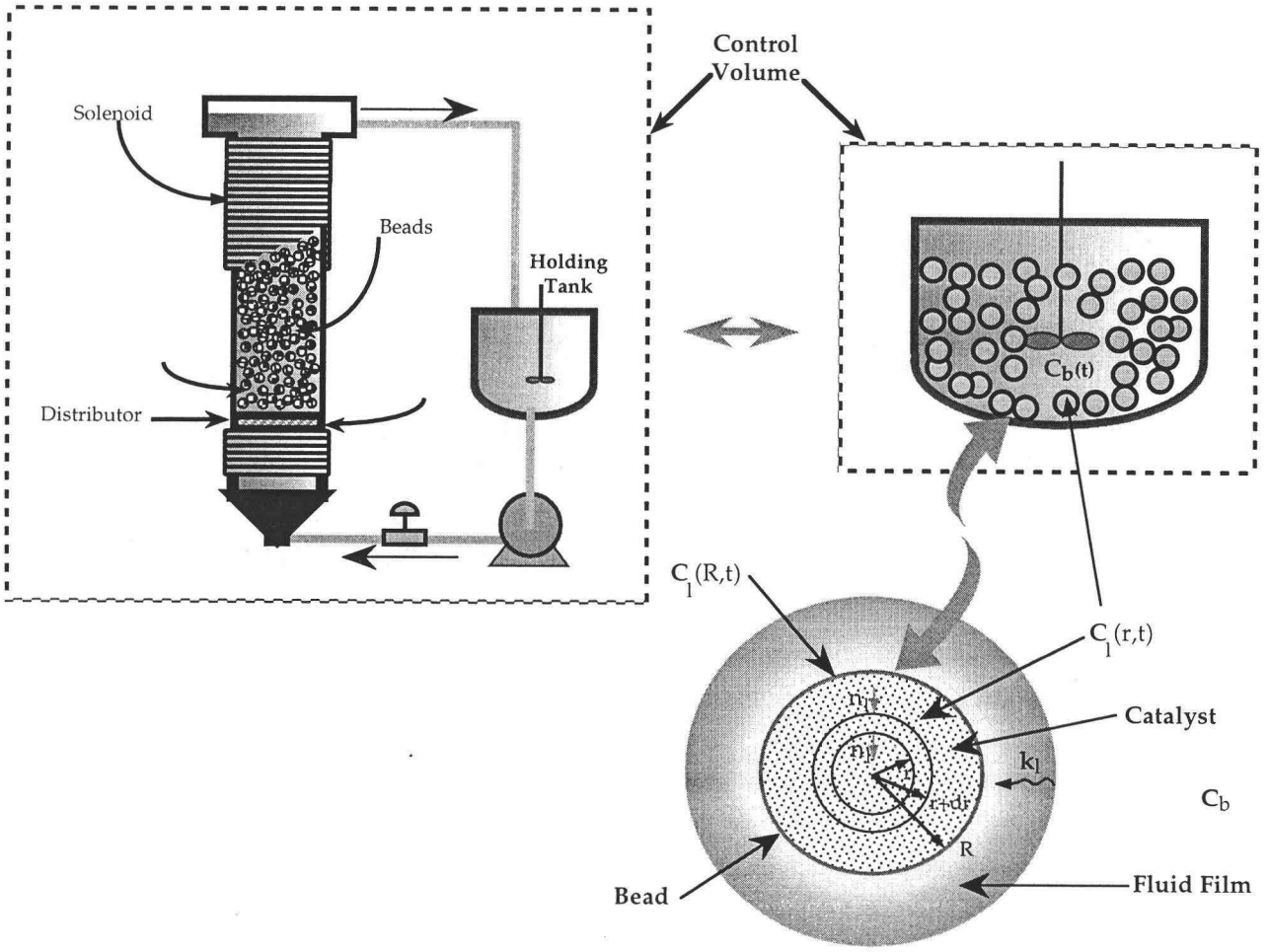

Figure 2.4 MSFB dechlorination reaction reactor system

A differential mass balance of any compound within the liquid phase in the alginate bead is given by:

$$\frac{\partial C_l(r,t)}{\partial t} = D_e\left(\frac{\partial^2 C_l(r,t)}{\partial r^2} + \frac{2}{r}\frac{\partial C_l(r,t)}{\partial r}\right) - \frac{k^*}{V'_{bd}(1-\phi)} C_l(r,t) a^n \qquad (2.21)$$

The last term in Equation 2.21 represents the disappearance of the chlorinated organic as discussed in section 2.1.2.

The initial conditions of the bulk and bead liquid as well as the boundary condition for the center of the bead respectively are:

Bead Liquid: $C_l(r, t=0) = C_{l,0}$ (2.22)

Bulk Liquid: $C_b(t=0) = C_{b,0}$ (2.23)

At the center of the bead at all times: $\left.\frac{\partial C_l(r,t)}{\partial r}\right|_{r=0} = 0$ (2.24)

The boundary condition at $r = R$ for the alginate bead is:

$$D_e(1-\phi)\left.\frac{\partial C_l(r,t)}{\partial r}\right|_{r=R} = k_l\left[C_b(t) - C_l(R,t)\right] \qquad (2.25)$$

A mass balance on the bulk liquid concentration, $C_b(t)$, is related to the diffusion at the outer boundary and is given by:

$$\frac{dC_b(t)}{dt} = -k_l\frac{3}{R}\frac{(1-\varepsilon)}{\varepsilon}\left[C_b(t) - C_l(R,t)\right] \qquad (2.26)$$

The detail derivation of this model is shown in Appendix A.

A similar model was used in the study of dechlorination of p-chlorophenol in MSFB (Graham, 1998). Graham also demonstrated that the plug flow model under certain conditions can be equivalent to the CSTR model which is used in this study.

2.3 Magnetically Stabilized Fluidized Bed Technology

Fluid-particle mass transfer in a fluidized bed is an important transport phenomenon for the dechlorination reaction process investigated in this study. Particles in a conventional fluidized bed are subjected to three macroscopic forces: the gravitational force F_g, the drag force F_d, and the buoyancy force F_b. As soon as the drag force balances the other two forces, the particles are fluidized.

In a conventional fluidized bed with a given fluid and solid system, the only way to increase the mass transfer between particles and fluid is to increase the fluid velocity. However, the bed will readily expand due to the increased fluid velocity. This cause the voidage, ε , to increase when the fluid velocity is increased. As a result the fluid interstitial velocity(u_{int}= u/ ε), which is the relative velocity between the particles and fluid, does not change since the voidage, ε , and the fluid velocity, u, are coupled and have opposite effects. Therefor the mass transfer coefficient, which depends strongly on interstitial velocity, u_{int}, will not change substantially.

In MSFB, however, an additional force is created by applying the magnetic field on particles containing ferromagnetic material. The particles are magnetized in the magnetic field. This results in two types of forces acting on the fluidized particles; the interparticle forces and the magnetic force from the magnetic field. The induced partical-partical force tends to bring particles together, which results in a decrease of the bed voidage, ε . The application of a non-uniform magnetic field creates an additional magnetic force within the bed. This new macroscopic force which is acting on the particles has to be overcome by the drag force. Hence, the fluid velocity through the bed has to be increased to compensate for this new force. Consequently, in a MSFB we can increase the fluid velocity and still maintain low bed voidage. This means that the interstitial velocity can be increased as well as the mass transfer coefficient. Figure 2.5 illustrates the previous discussion.

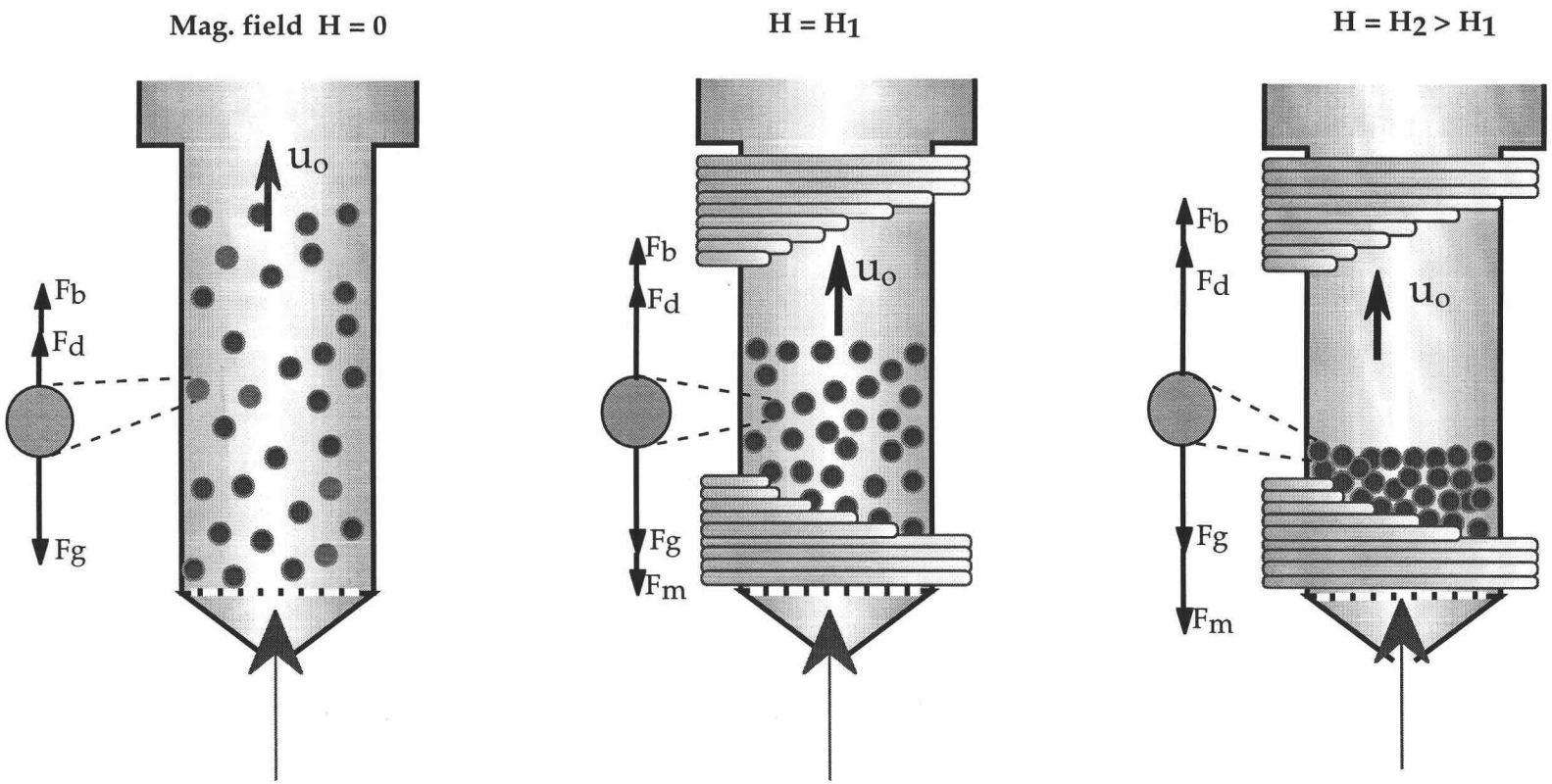

Figure 2.5 Illustration of effect of the magnetic field on fluidized particles in MSFB

Al-Mulhim (1995) presented the experimental result related to the enhancement of the mass transfer coefficient in a MSFB. He studied the mass transfer coefficient for different fluid velocities and different magnetic field intensities. A correlation, which can predict from the enhanced mass transfer coefficient in a MSEB in the presence of a homogenous magnetic field was also provided.

$$Sh = \frac{0.054}{[\varepsilon_o - mx_{wt}H]^2} \quad \frac{r^{0.67}u_o d_b}{m^{0.67}D_{AB}0.33} \tag{2.27}$$

also, $$Sh = \frac{k_l d_b}{D_{AB}} \tag{2.28}$$

$$k_l = \frac{0.054\, u_o}{[\varepsilon - mx_{wt}H]^2} Sc^{0.67} \tag{2.29}$$

However, the magnetic field applied to the MFSB system in this study was a non-homogeneous magnetic field.

The correlations used to determine the liquid–solid mass transfer coefficient in ordinary fluidized bed are reported respectively by Coderc *et. al* (1972), Fan *et. al* (1960) and Cussler (1984) :

$$Sh = \frac{0.054}{\varepsilon^2} Re\, Sc^{0.33} \tag{2.30}$$

$$Sh = 2 + 1.51(1-\varepsilon)\, Re^{0.5}\, Sc^{0.33} \tag{2.31}$$

$$k_l = 2.0 + 0.6\, Re^{0.5}\, Sc^{0.33} \tag{2.32}$$

with $$Re = \frac{\rho_l u_l d_b}{\mu_l} \tag{2.33}$$

and $$Sc = \frac{\mu_l}{\rho_l D_{AB}} \tag{2.32}$$

$$Sh = \frac{k_l d_b}{D_{AB}} \tag{2.33}$$

CHAPTER 3

EQUIPMENT, MATERIAL AND METHOD

3.1 Equipment

3.1.1 *Batch Reactor*

A Pd/Fe catalyst in powder form (not entrapped in alginate beads) is used in a batch reactor for the experimental measurement of the rate of dechlorination reactions. All reaction rate constants for the dechlorination of 2,4,6-trichlorophenol were obtained in the reaction system which is illustrated in Figure 3.1. A variable speed mixer was applied to continuously stir the solution and keep the catalyst powder suspended. In addition, a pH controller, a HCl supply system, and an N_2 supply line were also applied for controlling the pH and maintenance of the deoxygenated environment.

3.1.2 *Alginate Bead Generator*

The alginate bead generator is shown in Figure 3.2. it consists of a pressurized vessel, extrusion needle, air supply to the needle tip, and a catch beaker filled with calcium chloride. The 1.5 [w/w %] alginate solution was made before start to make beads. The solution is added to the pressurized vessel whereby it flows downward to the tip of the needle. The air supplied here allows for control of the particle size through control of the shear force. The bead drops into the catch beaker containing 1.0 [M] $CaCl_2$. The preparation of the 1.5 [w/w %] alginate solution and Pd/Fe catalyst entrapment is described in further detail in Appendix C.

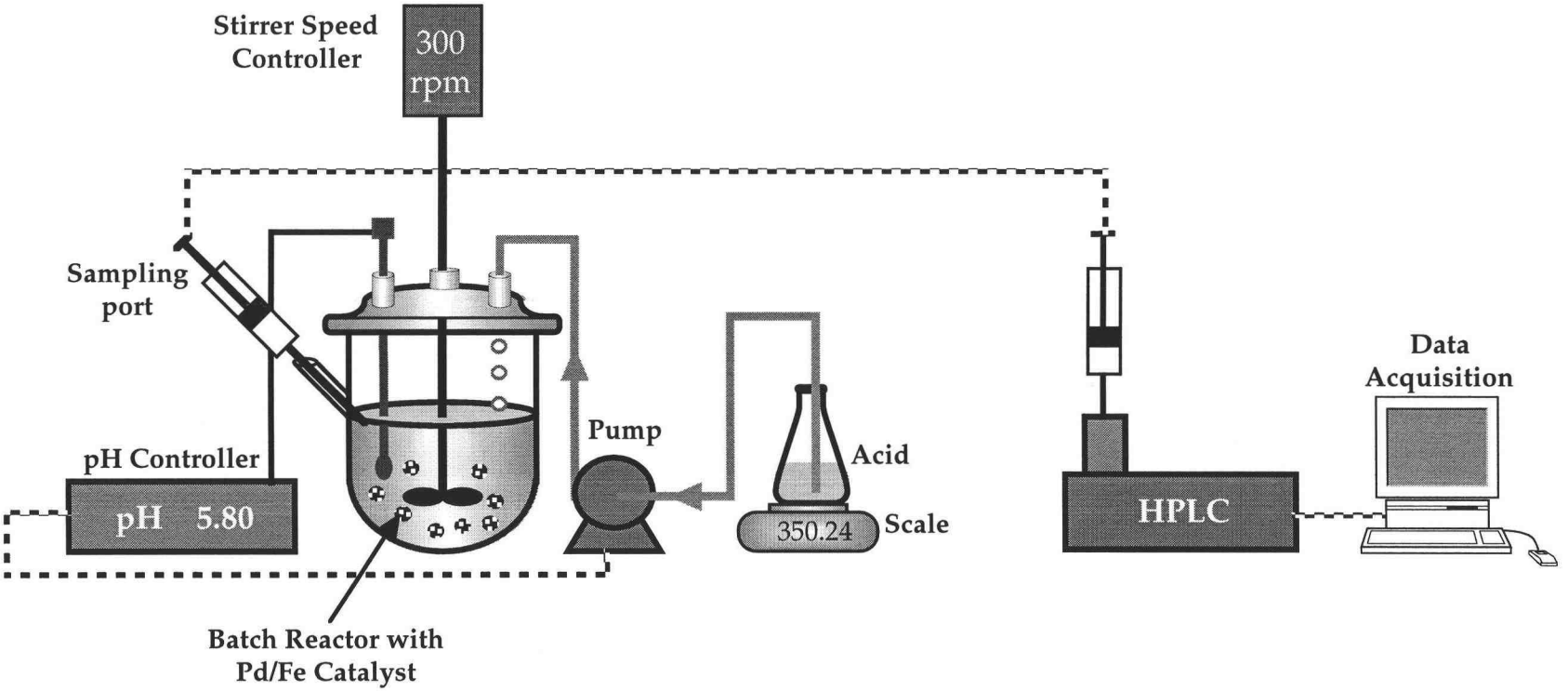

Figure 3.1 Chemical kinetic apparatus

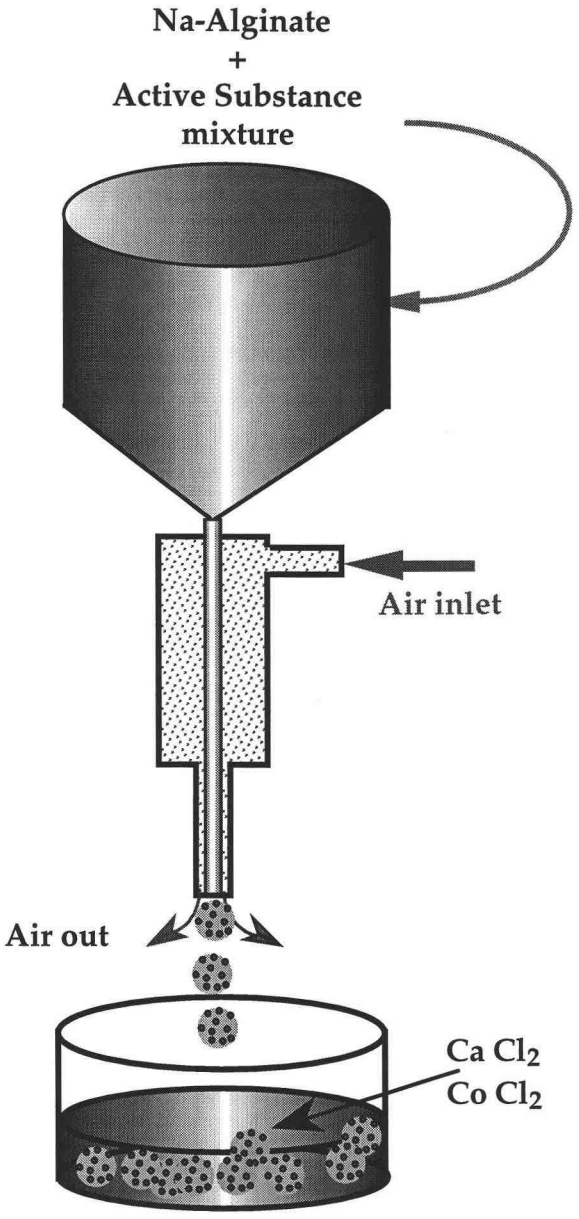

Figure 3.2 Alginate beads generator

3.1.3 MSFB Apparatus

The MSFB equipment used in this investigation is shown in Figure 3.3. The reactor column is 45 [cm] in height with a 3.8 [cm] inner diameter (i.d.) and 5.1 [cm] outer diameter (o.d.). The magnetic field is generated by wrapping copper wire (d_{wire} = 1 [mm]) around an acrylic tube. The coil consists of three layers of copper wire concentrically wrapped to varying heights which provides flexibility in generating a gradient magnetic field. A Masterflex peristaltic pump with tygon tubing recycles the liquid throughout the bed. An overflow box allows insertion of a pH probe to monitor pH, acid addition, and sample taken during the experiment. All liquid is deoxygenated and an N_2 inlet prevents air from reaching the fluid thus maintaining deoxygenated conditions.

3.2 Materials

3.2.1 *Properties of Chlorophenols*

2,4,6-trichlorophenol (purity: 98%) and 2,6-dichlorophenol (purity: 99%) were obtained from Alfa Aesar Chemical Company. 2,4-dichlorophenol (purity: 99%) and 2-chlorophenol (purity: 99+%) were obtained from Aldrich Chemical Company. 4-Chlorophenol was obtained from Acros Organics (purity: 99+%) and phenol (purity: 98.5%) was obtained from Baker Chemical Company. All of the chlorophenols are solid at room temperature, except 2-monochlorophenol, which is a liquid. The physical properties of these chlorophenols are listed on Table 3.1.

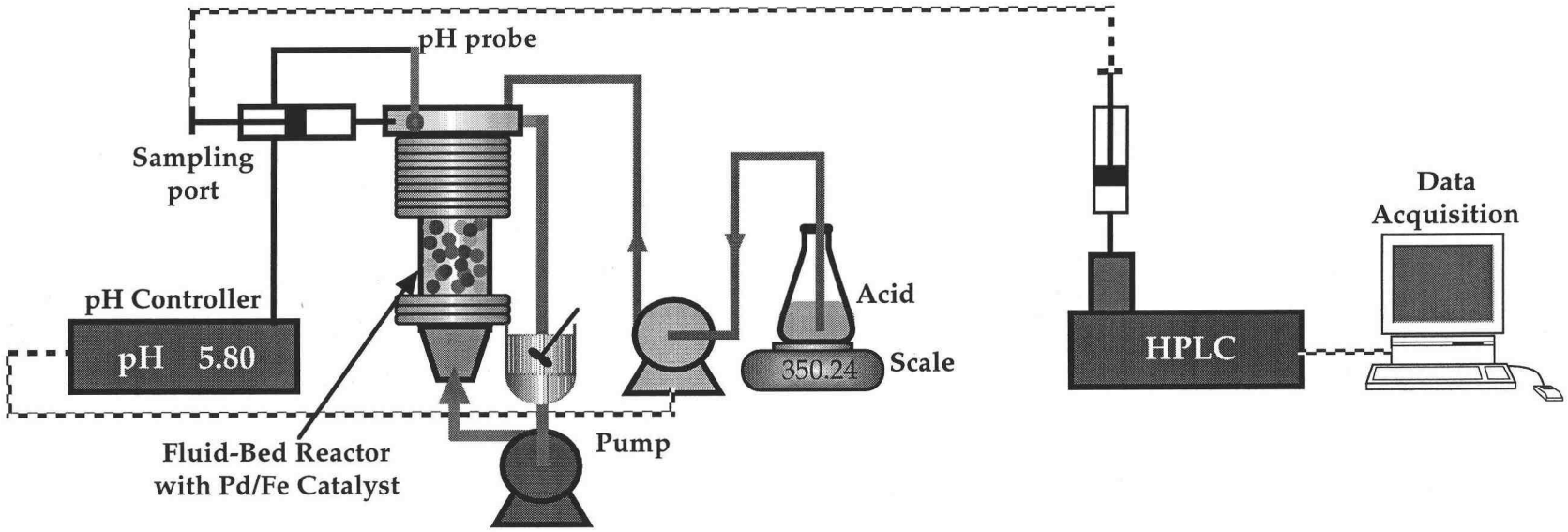

Figure 3.3 MSFB apparatus

Table 3.1 Physical Properties of Chlorophenols

Compound	Chemical Formula	Molecular Weight (g/mol)	Density	Boiling Point (°C at 760 mmHg)	Melting Point (°C at 760 mmHg)	Flash Point (°C)	Vapor Pressure (mmHg) (temperature)
Phenol	C_6H_6O	94.11	1.071	182	43	79	
p-chlorophenol	4-ClC_6H_4OH	128.56	1.2651	219.75	43.2-43.7	121.1	1 (49.8 °C)
o-chlorophenol	2-ClC_6H_4OH	128.56	1.2634	174.9	9	63.9	1 (12.1 °C)
an2,4- dichlorophenol	2,4-$Cl_2C_6H_3OH$	163	1.38	210	45	62	1 (76.5 °C)
2,6-dichlorophenol	2,6-$Cl_2C_6H_3OH$	163	---	219-220	68-69	---	1 (59.5 °C)
2,4,6-trichlorophenol	2,4,6-$Cl_3C_6H_2OH$	197.45	1.49	246	69.5	113.9	---

3.2.2 *Pd/Fe Catalyst*

The iron powder used for the manufacturing of catalyst was obtained from Aldrich Chemical Company in the size range of 5-8 [μm]. The palladium was obtained from Aldrich Chemical Company in the form of a salt, hexachloropalladate (K_2PdCl_6). The iron powder was pretreated with a 6 [M] HCl for five minutes and rinsed with three 25 [ml] aliquots of deionized water. The hexachloropalladate (K_2PdCl_6) was dissolved into deionized water before palladization process. The iron was then added to the hexachloropalladate solution and was mixed vigorously for 15 minutes. The palladized iron was then rinsed with 50 [ml] of deionized water. SEM were taken which show acid treated iron particles prior to palladization as well as after palladization when nano-size palladium islets can be easily identified. (Figure 3.4a,b). More details of the preparation of the Pd/Fe catalyst are given in section 3.3.1.

3.2.3 *Alginate*

Sodium alginate was donated by Kelco Company under the trademark name, Keltone HV (Keltone Product, 1996). Keltone HV is derived from a giant brown kelp, *Macrocystis pyrifera*, and consists of alternating D-mannuronic and L-guluronic acid units. When dissolved in distilled water, a solution is prepared whose flow characteristics are affected by shear rate, polymer size, temperature, concentration in

a)

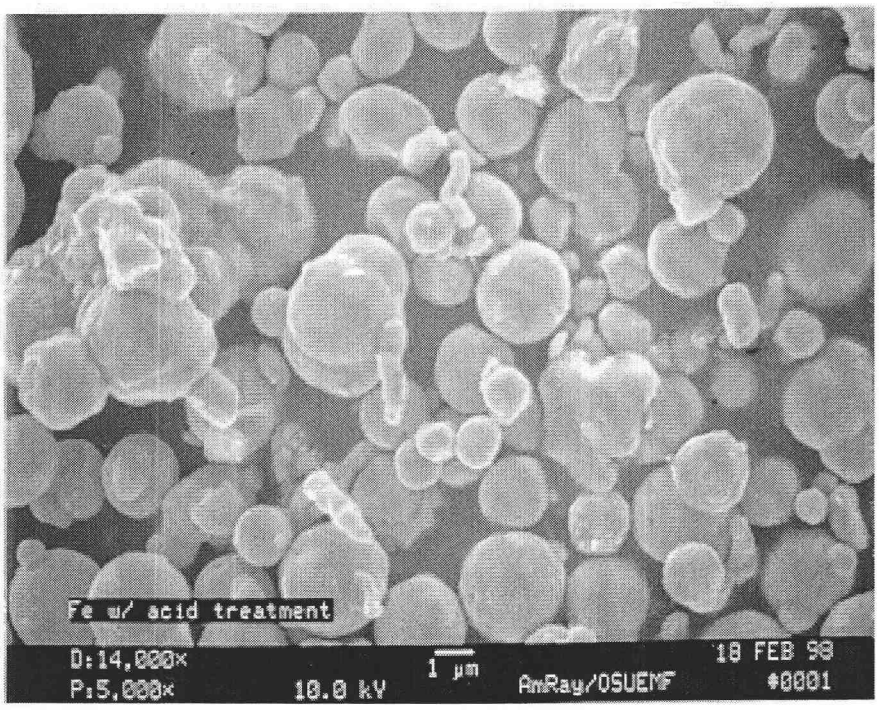

b)

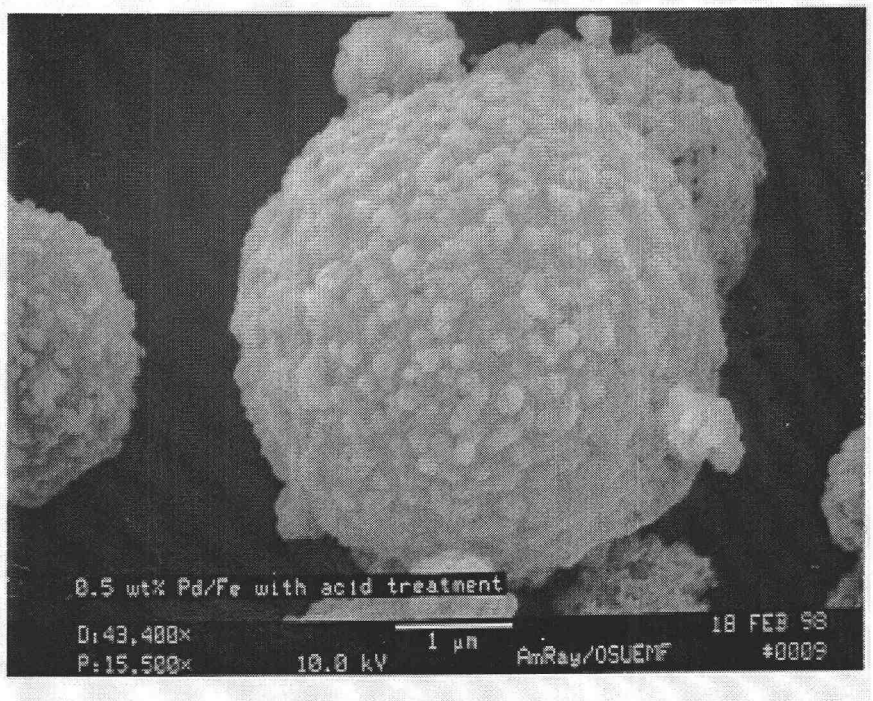

Figure 3.4 Scanning electron microscopy pictures:
a) Acid pretreated Fe particles, b) Palladized Fe particles

solution and the presence of miscible solvents. For all experimental work in this study, a 1.5 [%] solution of algin and 98.5 [%] distilled water was prepared at room temperature before any active substance was added for entrapment (Appendix C).

3.2.4 *Surfactant*

Since the solubility of 2,4,6-trichlorophenol in water is fairly low, the surfactant was used to increase the solubility of 2,4,6-trichlorophenol. A study (Abdul et al, 1990) of selection of surfactants for the removal of petroleum products from shallow sandy aquifers has reported that three surfactants, Witconol 1206, Witconol SN70, and Witconol SN90, have good potential for the effective in-situ washing of petroleum products and hydrophobic organic contaminates from soil. It was also pointed out that Witconol SN70, which was chosen for this study, has better detergency and solubilization potential.

Witconol SN70, an ethoxylated alcohol, was obtained from Witco Corporation. It is a clear, colorless liquid, specific gravity (at 25°C) is 0.98, pH in water solution is 6 to 8, and average molecular weight(g/mol) is 392. An 1%(w/w) solution of Witconol SN70 in water is used in this study.

3.3 Methods

3.3.1 *Preparation of Pd/Fe Catalyst*

The production procedure for the preparation of the Pd/Fe catalyst is described below:

1. Weigh 6.0[g] iron powder, rinse with 25[ml] of deionized water twice.
2. Wash the iron powder with 25[ml] of 6[M] HCl for 5 minutes to remove surface oxide layers, then rinse with 25[ml] of deionized water three times.
3. Weigh 0.045[g] hexachloropalladate (K_2PdCl_6) and dissolve it in 250[ml] deionized water.
4. Add the hexachloropalladate solution into the iron powder, stir with glass stir rod for 15 minutes. This will give a 0.02-0.75[w/w%] palladium coverage. The reaction of forming palladium iron is as follows

   $Pd^{4+}+2Fe^0 \rightarrow Pd^0+2Fe^{2+}$

   The reaction is considered complete when the dark orange solution of hexachloropalladate (K_2PdCl_6) turns to a pale yellow.
5. Rinse the palladium iron catalyst with 25[ml] deionized water three times.

3.3.2 *Determination of the Concentration of Chlorophenols*

High-pressure liquid chromatography (HPLC) is used to determine the concentration of chlorophenols in the reaction solution. The HPLC contains a pump to deliver the mobile phase, a 20[μL] sample loop sample injector, a LC-8 column

from Supelco with reverse phase silica gel packing, and a Gilson UV detector set to a wavelength 280[nm]. Mobile phase which consists of 70[%] acetic-acid methanol solution (1% acetic-acid, 99% HPLC grade methanol) and 30[%] acetic-acid deionized water solution (1% acetic-acid, 99% deionized water) is used for determining the concentration of 2,4,6-trichlorophenol and 2,4-dichlorophenol. Mobile phase which consists of 55[%] acetic-acid methanol solution (1% acetic-acid, 99% HPLC grade methanol) and 45[%] acetic-acid deionized water solution (1% acetic-acid, 99% deionized water) is used for determining the concentration of 2,6-dichlorophenol, 4-chlorophenol, 2-chlorophenol, and phenol. The instrument is calibrated using several known concentration of chlorophenols. Peak areas were checked for each chlorophenol and linear relationship between the concentration of each compound and peak areas were obtained (Appendix B). Figure 3.5 and 3.6 illustrate the chromatogram of the HPLC analysis.

3.3.3 *Experimental Determinationof the Dechlorinnation Rate Constants*

Experiment are performed in a batch reactor as described in section 3.1.1. Six grams of Pd/Fe catalyst are prepared as described in section 3.3.1. 200[ml] solution of known initial concentration of cholorphenol is added into the batch reactor and mixed at 300[rpm] mixing rate.

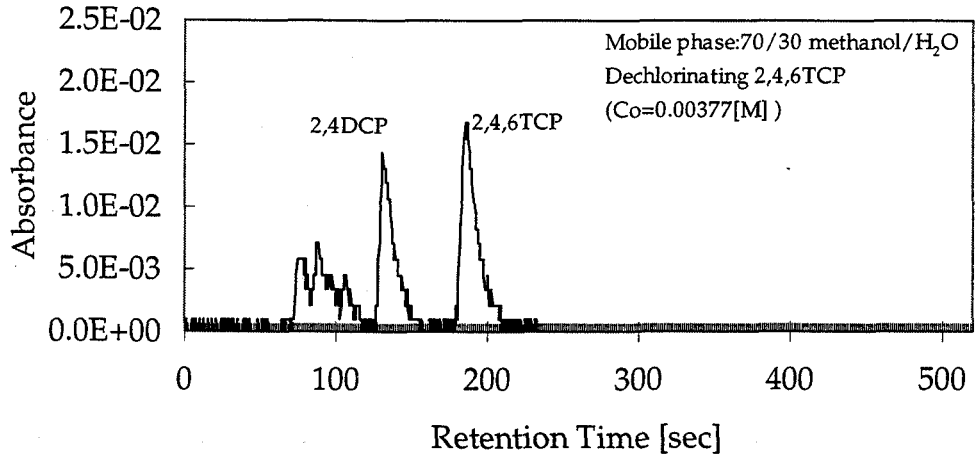

Figure 3.5 Chromatogram of HPLC Analysis

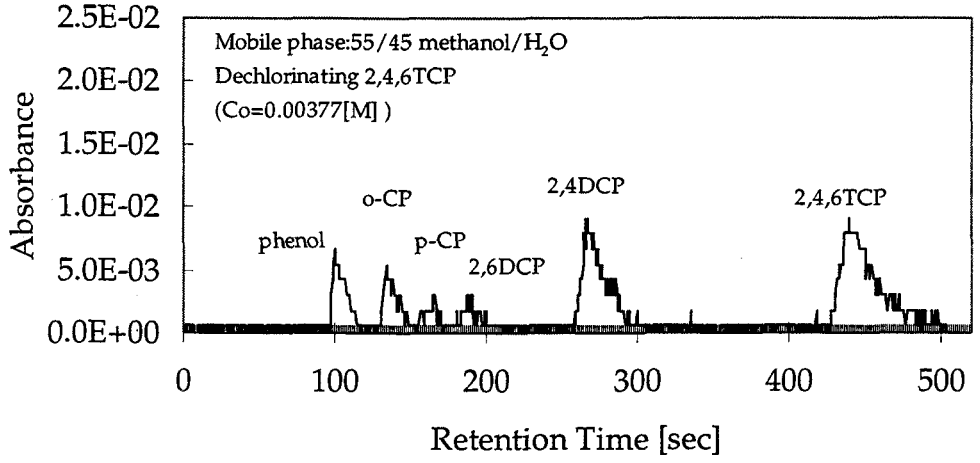

Figure 3.5 Chromatogram of HPLC Analysis

The influence of the mass transfer resistance between the bulk liquid and catalyst surface to the dechlorination reaction rate in the same reactor system has been investigated (Graham, 1998). A series of experiments were run over a range of mixing speeds (100-350 [rpm]) until the dechlorination curve was no longer dependent upon the impeller speed. The results show that between 100 and 150 [rpm], significant increase in the rate was observed. However, as mixer speed increased from 250-350 [rpm], little change was observed. In this study, the mixing rate is set at 300[rpm] for all the experiment performed in this batch system to prevent from this interference.

In order to avoid the effect of the formation of iron hydroxide on the catalyst surface, all experiments were run under deoxygenated condition and controlled pH at 5.7. Samples are taken at appropriate time intervals and are centrifuged after being taken out from the batch reactor. The sample solution is separated from the catalyst particles to prevent further reaction in the sample test tube before being analysis. Results of these experiments are presented in Chapter 4.

3.3.4 *Dechlorination of the 2,4,6-trichlorophenol in the Fluidized Bed Reactor*

To illustrate the applicability of MSFB for these reaction processes, decloroination of 2,4,6-trichlorophenol are performed in a fluidized bed reactor with and without external magnetic field. Known initial concentration 2,4,6-

trichlorophenol solution was added into the fluidized bed reactor system. 0.188[w/w%] Pd/Fe catalyst is prepared and alginate beads with this catalyst are produced as described in Appendix C. The beads are introduced into the reaction column and the pump is set at desired flow rate. The pH was monitored by a pH probe integrated with the pH controller. HCl acid is added for the control of the pH level at 5.7 during the experiment. Samples are taken at desired time intervals from the overflow box and analyzed in HPLC to determine the concentration of chlorophenols. Results of these experiments are described in Chapter 4.

CHAPTER 4
EXPERIMENTAL DATA

4.1 Dechlorination of Chlorophenols with Powdered Pd/Fe Catalyst

4.1.1 *Dechlorination of 2,4,6-trichlorophenol*

To determine the rate constants, the experiment of dechlorinating 2,4,6-trichlorophenol was run in a batch reactor as described in Chapter 3 for one hour. The initial volume of the reactor fluid was 200 ml 378.87ppm 2,4,6-TCP solution. Six grams of Pd/Fe (0.188%[w/w%] Pd) catalyst is used in this experiment, the pH was controlled at 5.7, and the mixer was set at speed of 300 RPM. Samples were saved for HPLC analysis to determine the concentration of 2,4,6-trichlorophenol and 2,4-dichlorophenol by using mobile phase methanol to water ratio 70 to 30 and the concentration of 2,6-dichlorophenol, p-chlorophenol, o-chlorophenol, and phenol by using mobile phase methanol to water ratio 55 to 45. The volume of the reactor changed due to the addition of acid and samples extraction. Figure 4.1 shows the volume change of the reactor fluid versus reaction time.

The concentration of 2,4,6TCP, 2,4DCP, 2,6DCP, 4CP, 2CP, and phenol were measured as the reaction proceeds in time. Figure 4.2 shows the mass balance of this reaction.

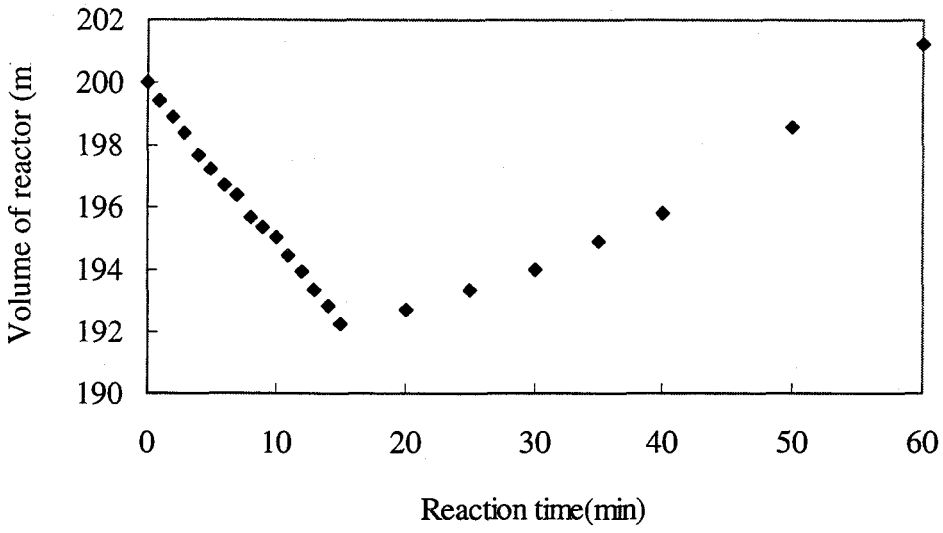

Figure 4.1 Volume change in dechlorination of 2,4,6-TCP

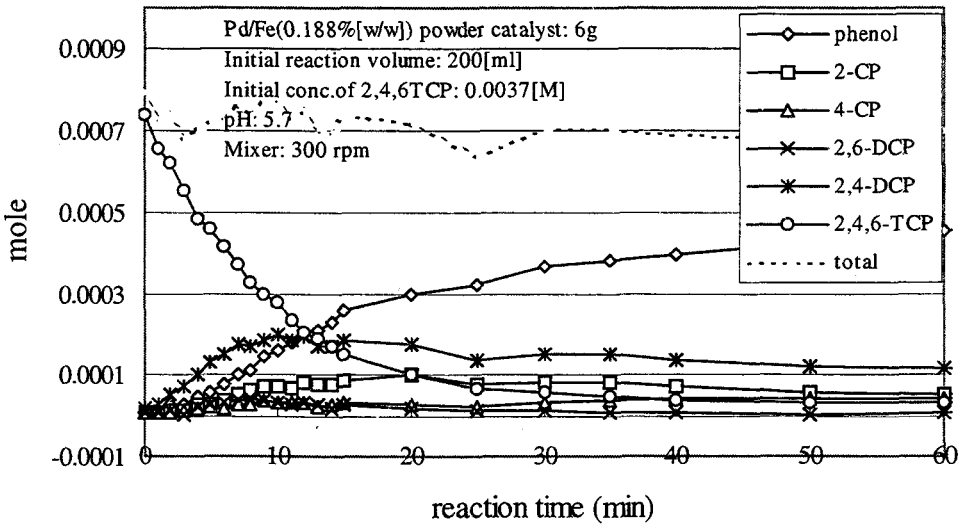

Figure 4.2 Total mass balance in dechlorination of 2,4,6-TCP

4.1.2 *Dechlorination of Dichlorophenol*

As shown in figure 4.2, the concentration of the intermediates such as 2,4-DCP, 2,6-DCP, 4-CP, and 2-CP during the reaction process are much lower than the concentration of 2,4,6-TCP and phenol. In order to obtain more resolute information for determining the reaction rate constant, k_3, k_4, k_5, k_6, and k_7, two additional experiments are performed. The dechlorination of 2,4-DCP and 2,6-DCP are also performed in the batch reactor under the same condition as dechlorination of 2,4,6-TCP. Figures 4.3 to 4.6 show experimental data obtained in these reaction process.

4.1.3 *Dechlorination of p-Chlorophenol*

The concentration level of p-chlorophenol in the dechlorination of 2,4-dichlorophenol reaction was still not high enough to ensure accurate determination of the reaction rate constant k_6. Another experiment, dechlorination of p-chlorophenol is performed under the same condition to determine the reaction rate constant for the dechlorination of p-chlorophenol. Figures 4.7 and 4.8 show the volume change and the mass balance in this reaction respectively.

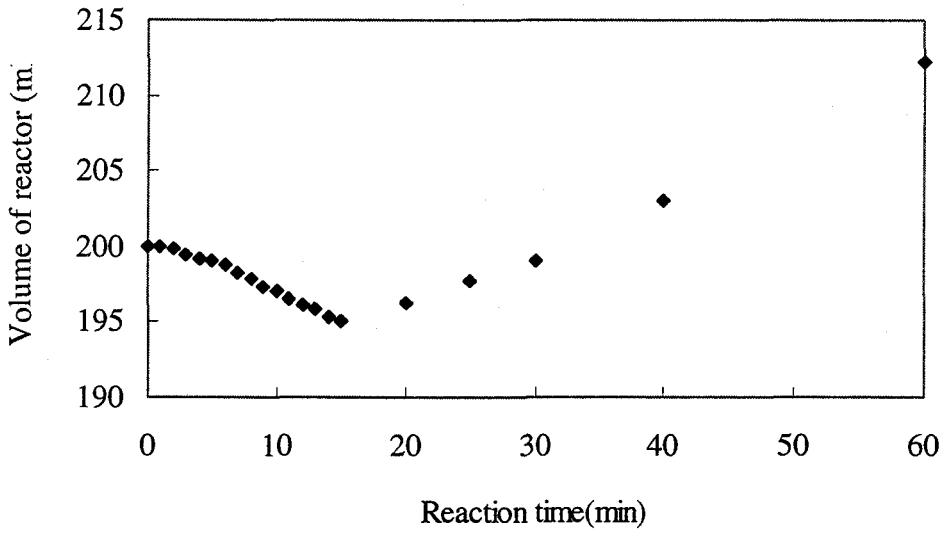

Figure 4.3 Volume change in dechlorination of 2,4-DCP

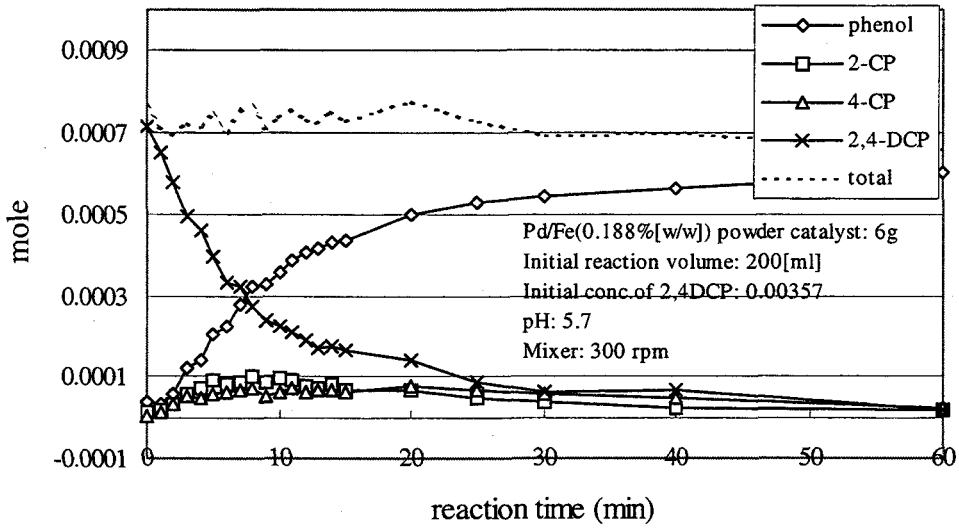

Figure 4.4 Total mass balance in dechlorination of 2,4-DCP

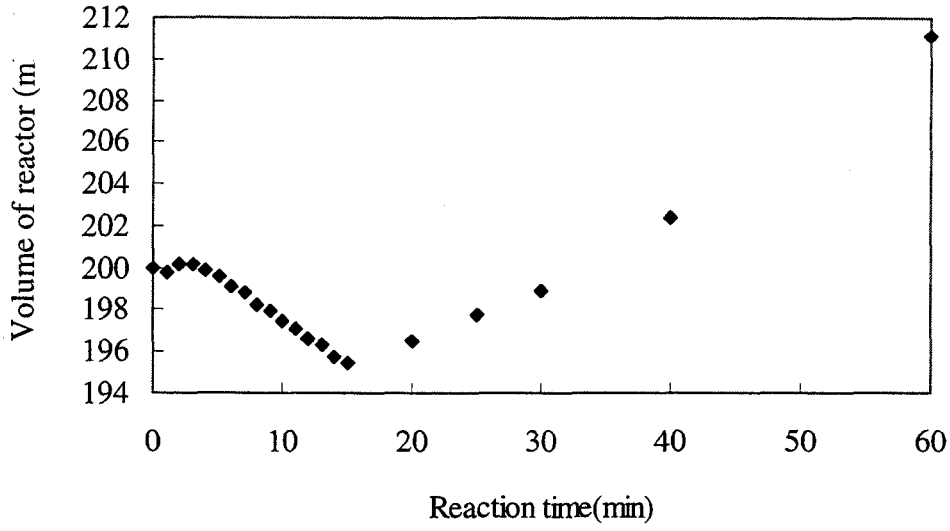

Figure 4.5 Volume change in dechlorination of 2,6-DCP

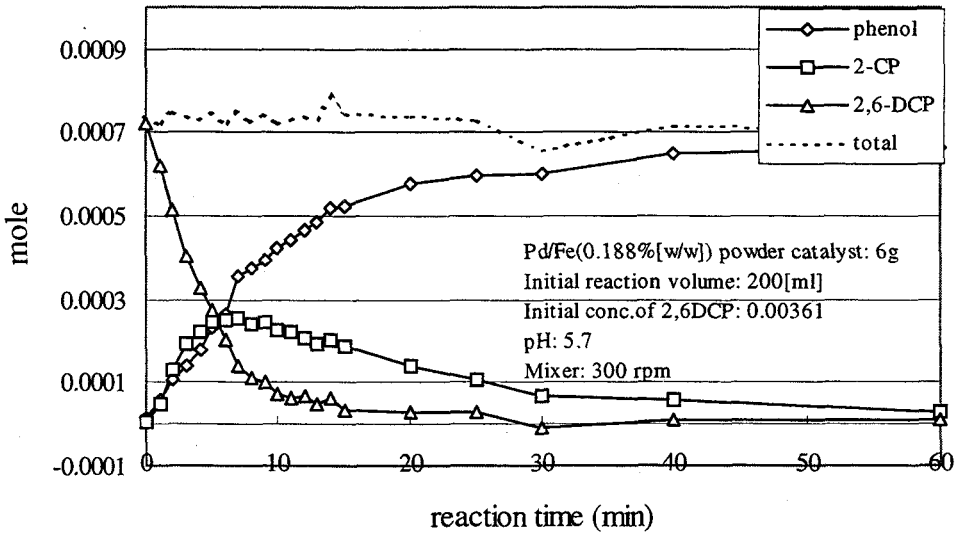

Figure 4.6 Total mass balance in dechlorination of 2,6-DCP

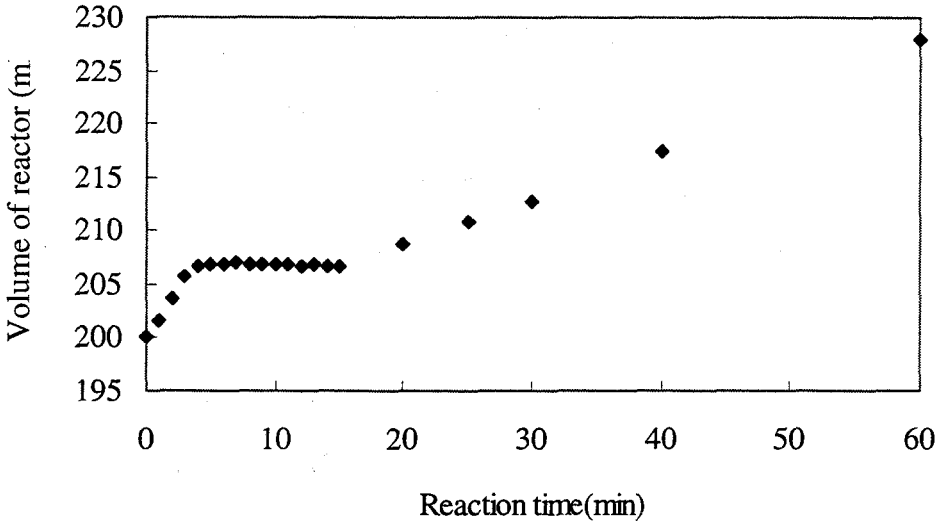

Figure 4.7 Volume change in dechlorination of p-chlorophenol

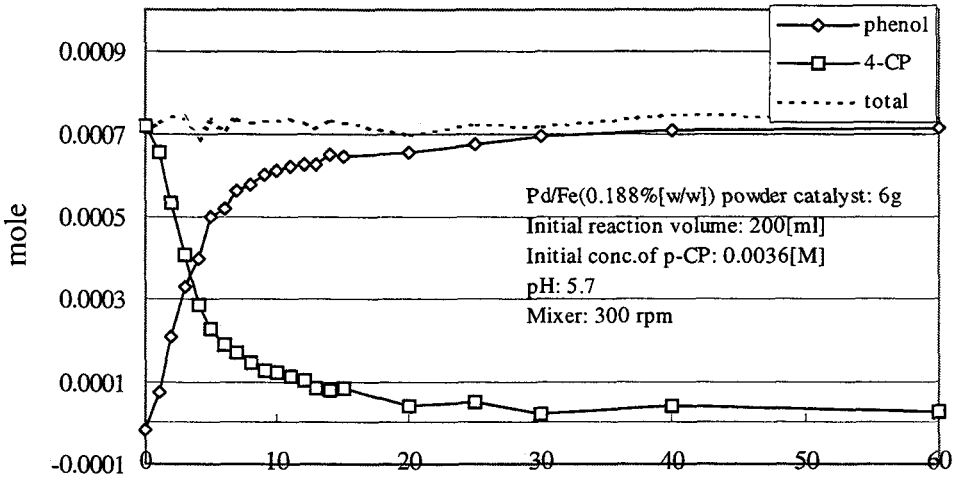

Figure 4.8 Total mass balance in dechlorination of p-chlorophenol

4.2 Dechlorination of 2,4,6-trichlorophenol in Fluidized Bed

The MSFB, integrated with the catalyst entrapped alginate beads, is shown as an engineering plateform for delivering catalytic action of the Pd/Fe catalyst. One advantage of the application of the magnetic field is the enhancement of the mass transfer between the bulk liquid and magnetically susceptible beads while aiding in the retention of beads within the fluidized bed. To illustrate the applicability of MSFB technology in the dechlorination of 2,4,6-trichlorophenol contaminated liquid, two experiment are performed in the MSFB system. Figure 4.9 and 4.10 represent the experimental data for without applying magnetic field and with applying the magnetic field respectively. Figure 4.11 shows the comparison of these tow run.

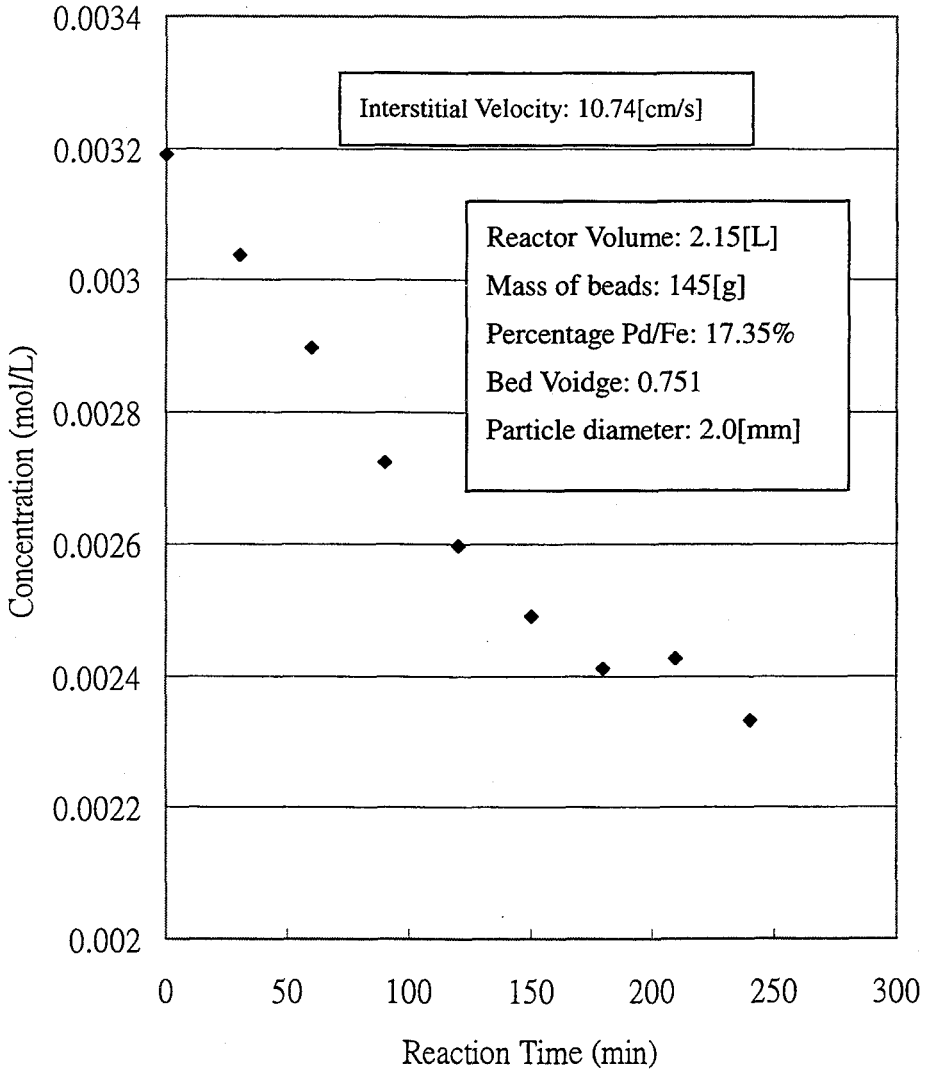

Figure 4.9 Dechlorination of 2,4,6-trichlorophenol with Entrapped Pd/Fe Catalyst in Fluidized Bed without Applied Field

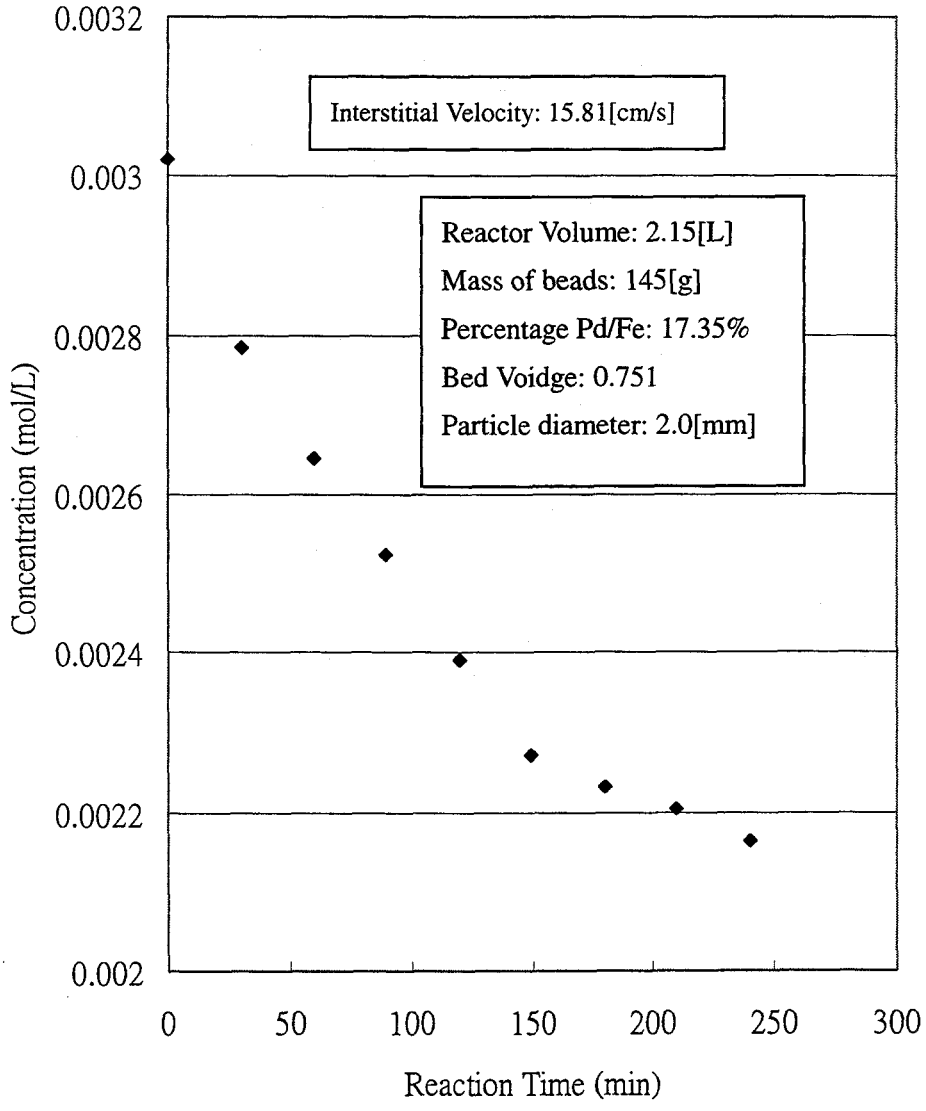

Figure 4.10 Dechlorination of 2,4,6-trichlorophenol with Entrapped Pd/Fe Catalyst in Fluidized Bed with Applied Field

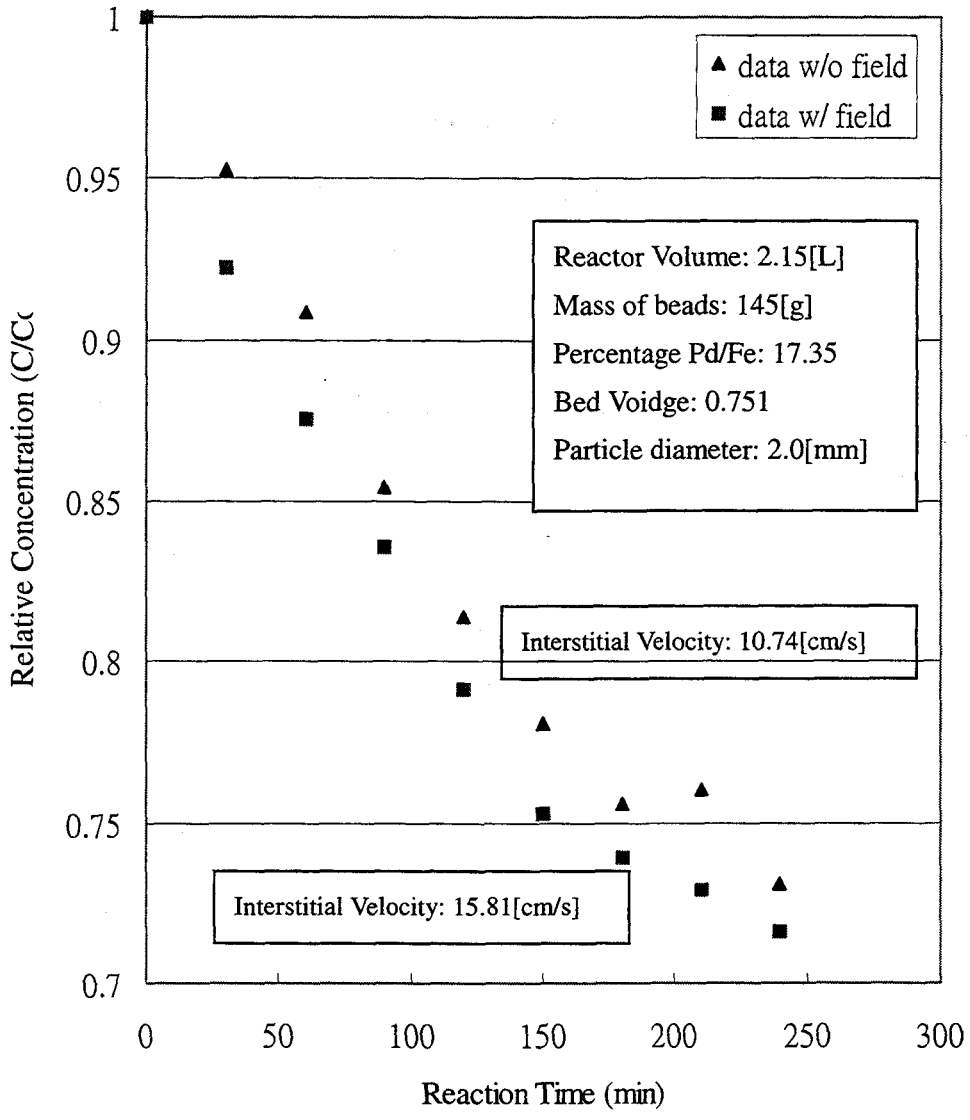

Figure 4.11 Comparsion of Dechlorination of 2,4,6-trichlorophenol in MSFB with and without Applied Field

CHAPTER 5

RESULT AND DISCUSSION

5.1 Dechlorination of the 2,4,6-trichlorophenol on the Pd/Fe Powdered Catalyst

The rate equations developed in section 2.2.2 (Equation 2.13 to 2.18) are solved simultaneously by using finite difference numerical methods. The reaction rate constants and the deactivation rate constant of 2,4,6-trichlorophenol dechlorination are determined. The volume change due to the addition of acid and removal of samples is also incorporated. Notice that when samples are extracted, not only the volume of the reactor is changed but the mass of all the chemical species in the reactor are changed as well. One term is added in the rate equation to compensats this mass balance effect as shown in Equation 5.1 to 5.6.

$$-\frac{d(VC_1)}{dt} = (k_1^* + k_2^*)C_1 a - FC_1 \tag{5.1}$$

$$-\frac{d(VC_2)}{dt} = (k_3^* + k_4^*)C_2 a - k_1^* C_1 a - FC_2 \tag{5.2}$$

$$-\frac{d(VC_3)}{dt} = k_5^* C_3 a - k_2^* C_4 a - FC_3 \tag{5.3}$$

$$-\frac{d(VC_4)}{dt} = k_6^* C_4 a - k_3^* C_2 a - FC_4 \tag{5.4}$$

$$-\frac{d(VC_5)}{dt} = k_7^* C_5 a - k_4^* C_2 a - k_5^* C_3 a - FC_5 \qquad (5.5)$$

$$-\frac{d(VC_6)}{dt} = -k_6^* C_4 a - k_7^* C_5 a - FC_6 \qquad (5.6)$$

Initial condition for these differential equations are:

$at \quad t=0,$

$$C_1=C_{1,0} \qquad (5.7)$$

$$C_2=C_3=C_4=C_5=C_6=0 \qquad (5.8)$$

A Fortran program utilizing IMSL subroutines was written to solve the differential equation and produce the model output bulk concentrations of all chemical species. An optimization routine UMCGF is also used to search for the reaction rate constants and the deactivation rate constant until the objective function, F_{obj}, as defined by Equation 5.7 reaches the minimum.

$$F_{obj} = \sum \left(C(t)_{model} - C(t)_{expt}\right)^2 \qquad (5.9)$$

The IMSL subroutines, Fortran program for solving the reaction rate constants and the deactivation rate constant, are shown in Appendix F.

The concentrations of every chemical component involved in the dechlorination process are then plotted for comparison. Figure 5.1 to 5.6 shows the experimental data and the model fit for every specie involved in the dechlorination of 2,4,6-trichlorophenol including 2,4,6-trichlorophenol, 2,4-dichlorophenol, 2,6-dichlorophenol, p-chlorophenol, o-chlorophenol, and phenol. Figure 5.7 to 5.10 illustrates the experimental data and modelfit for the dechlorination of 2,4-dichlorophenol obtained in a separate experiment. Figure 5.11 to 5.13 present the dechlorination of 2,6-dichlorophenol and Figure 5.14 and 5.15 show the dechlorination of p-chlorophenol all obtained in separate independent experiments.

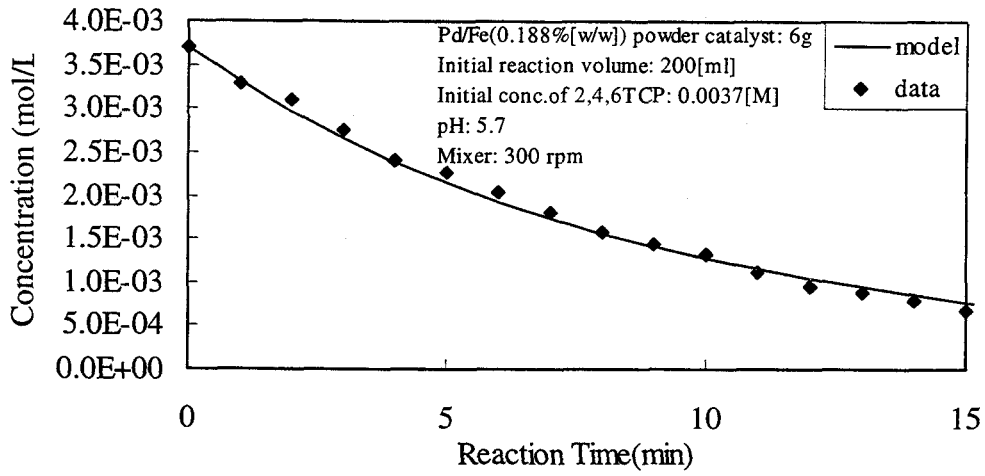

Figure 5.1 Comparison of 2,4,6-trichlorophenol concentration in dechlorination of 2,4,6-TCP with model output

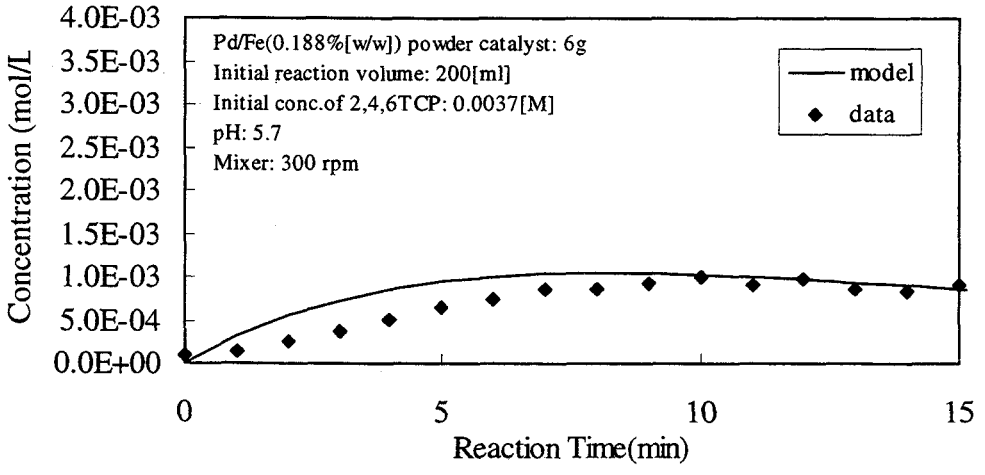

Figure 5.2 Comparison of 2,4-dichlorophenol concentration in dechlorination of 2,4,6-TCP with model output

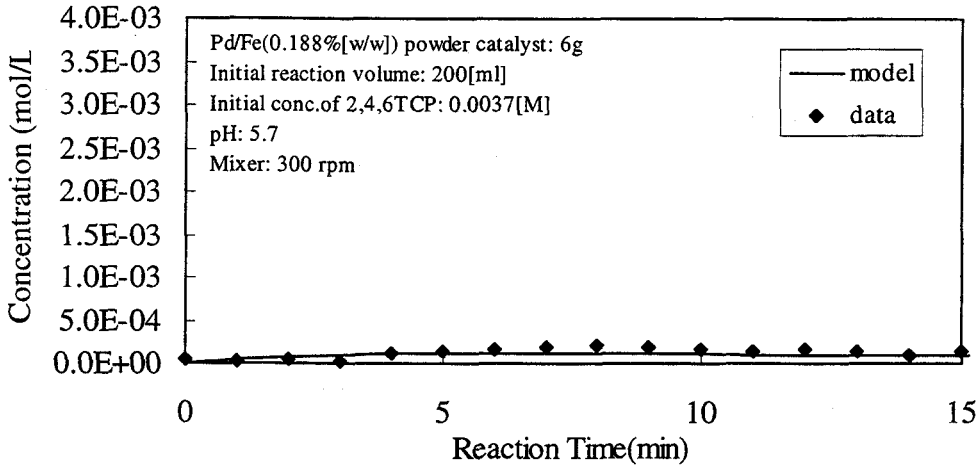

Figure 5.3 Comparison of 2,6-dichlorophenol concentration in dechlorination of 2,4,6-TCP with model output

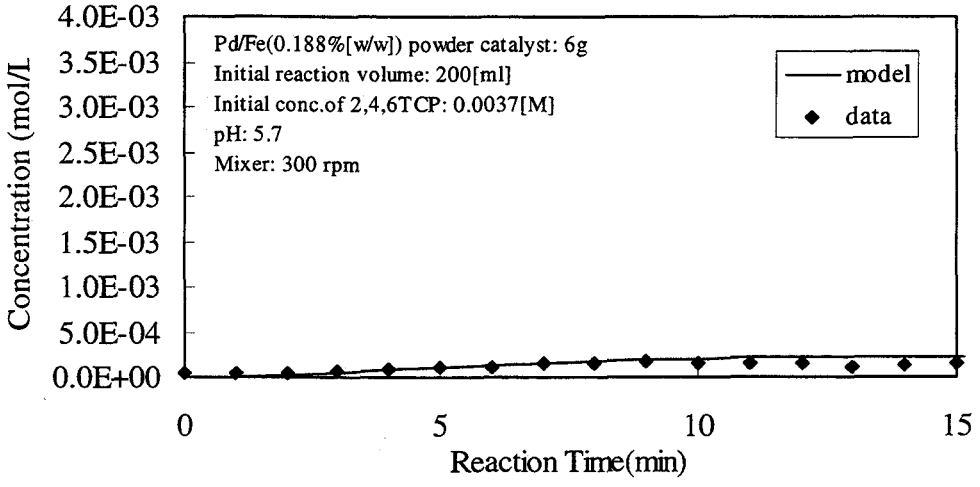

Figure 5.4 Comparison of p-chlorohenol concentration in dechlorination of 2,4,6-TCP with model output

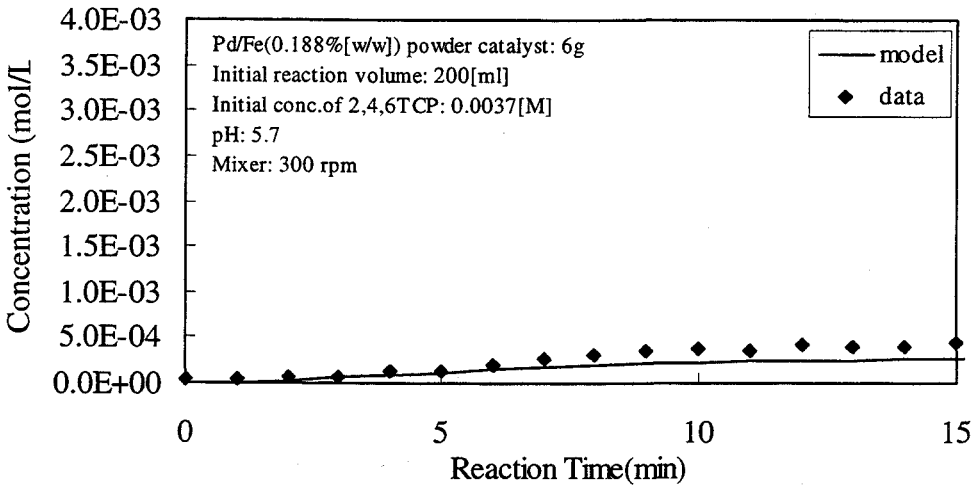

Figure 5.5 Comparison of o-chlorophenol concentration in dechlorination of 2,4,6-TCP with model output

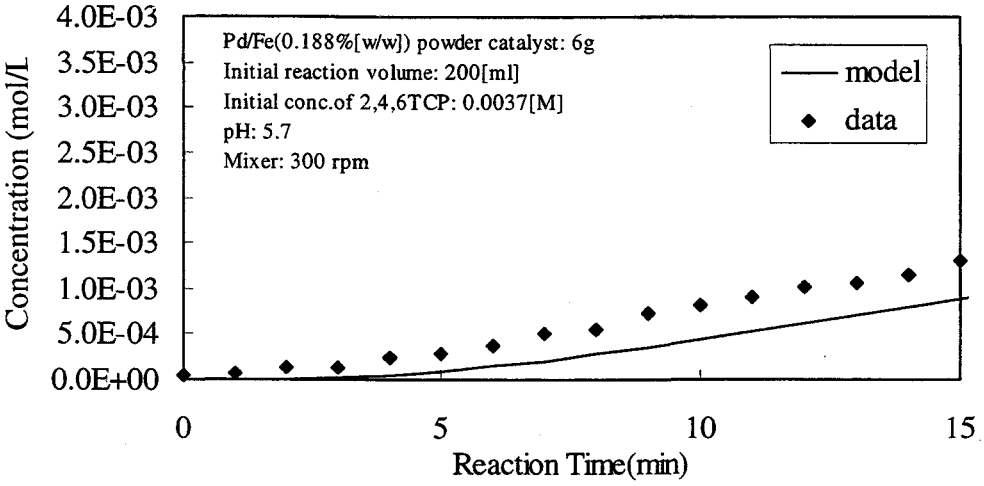

Figure 5.6 Comparison of phenol concentration in dechlorination of 2,4,6-TCP with model output

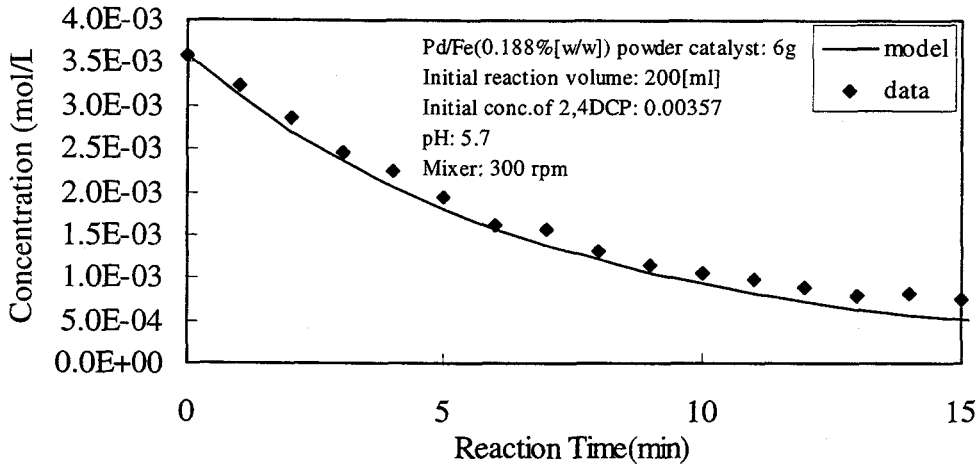

Figure 5.7 Comparison of 2,4-dichlorophenol concentration in dechlorination of 2,4-DCP with model output

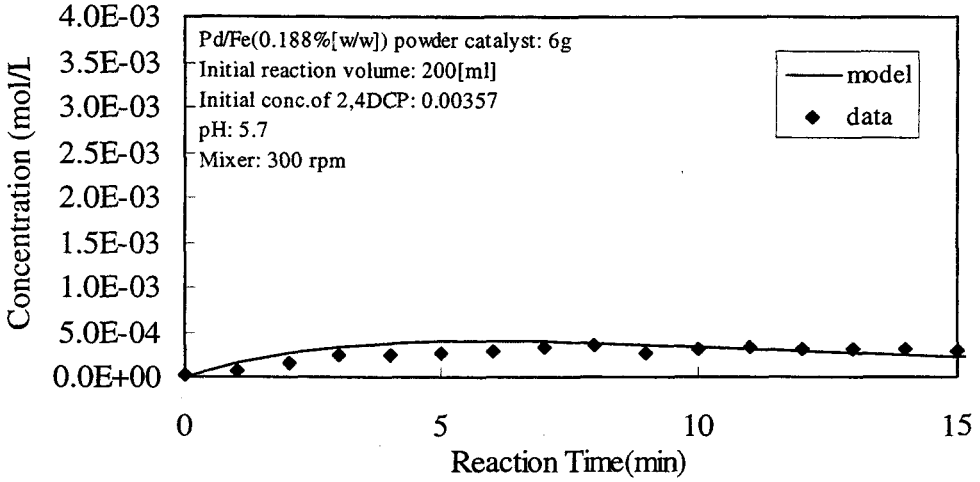

Figure 5.8 Comparison of p-chlorophenol concentration in dechlorination of 2,4-DCP with model output

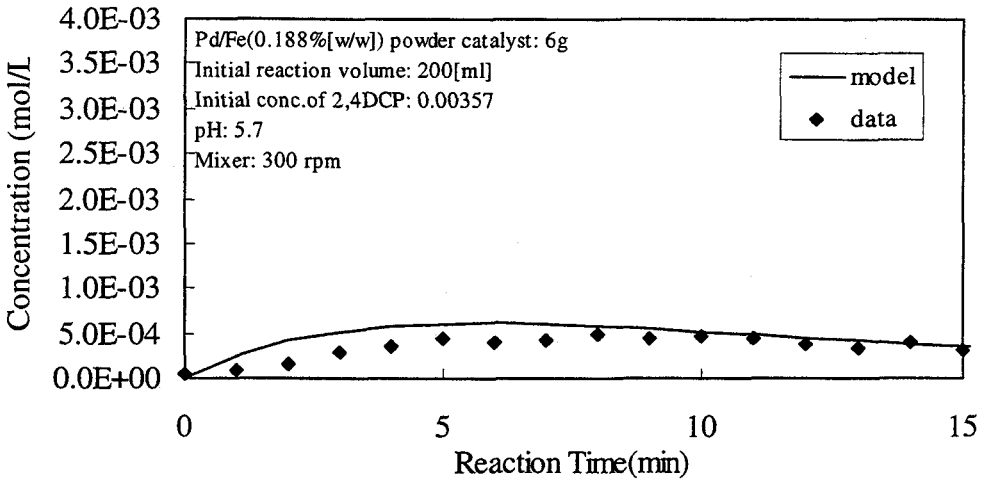

Figure 5.9 Comparison of o-chlorophenol concentration in dechlorination of 2,4-DCP with model output

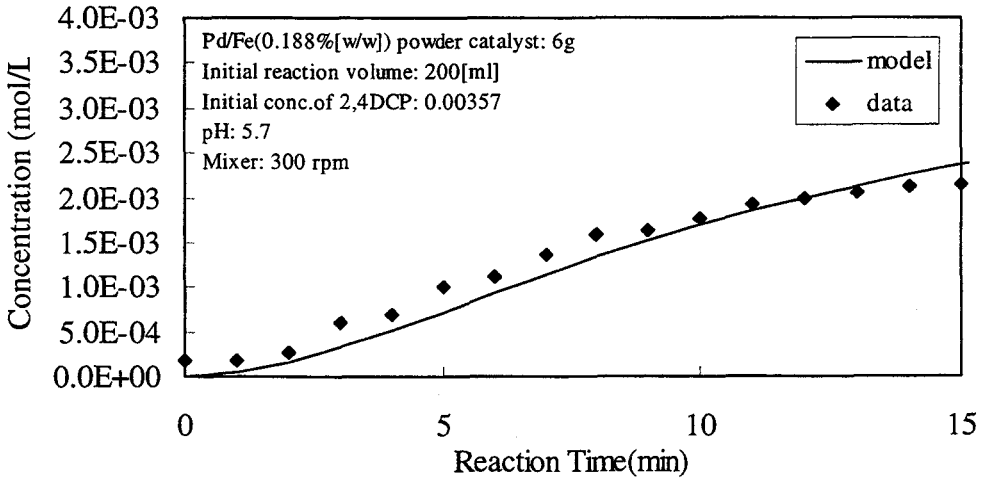

Figure 5.10 Comparison of phenol concentration in dechlorination of 2,4-DCP with model output

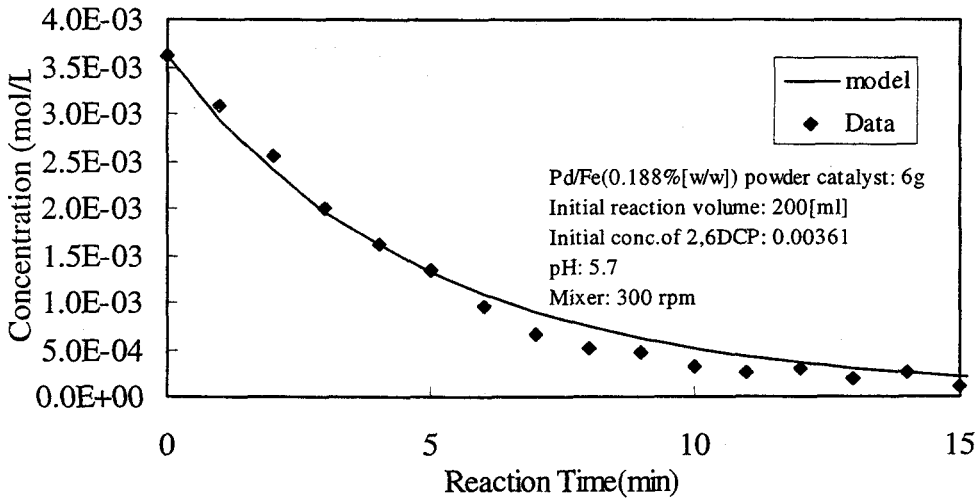

Figure 5.11 Comparison of 2,6-dichlorophenol concentration in dechlorination of 2,6-DCP with model output

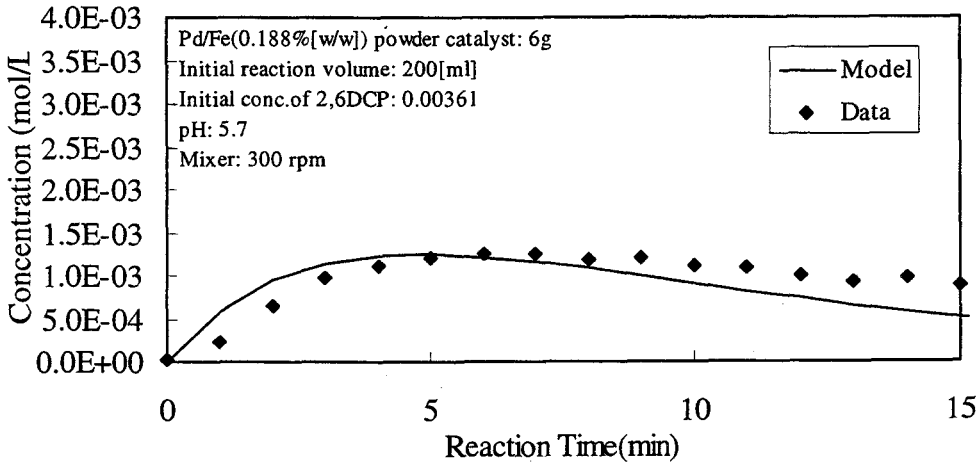

Figure 5.12 Comparison of o-chlorophenol concentration in dechlorination of 2,6-DCP with model output

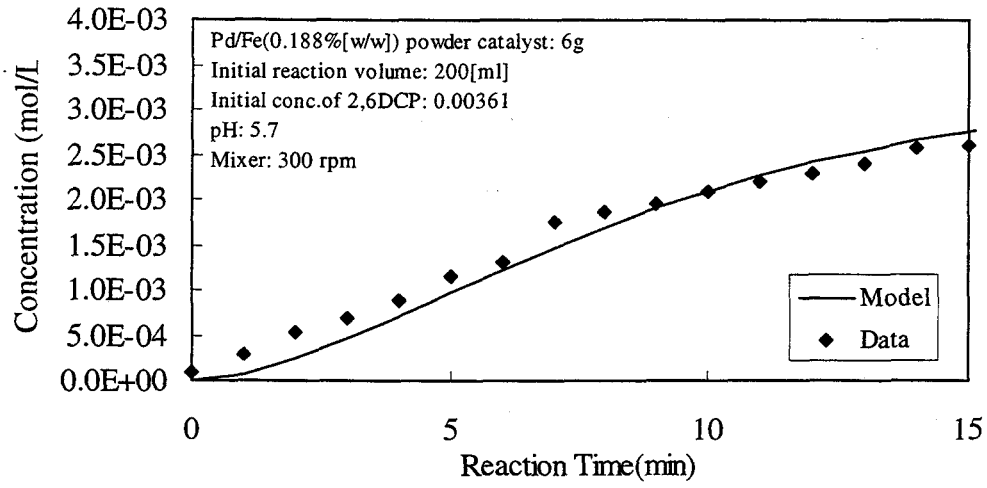

Figure 5.13 Comparison of phenol concentration in dechlorination of 2,6-DCP with model output

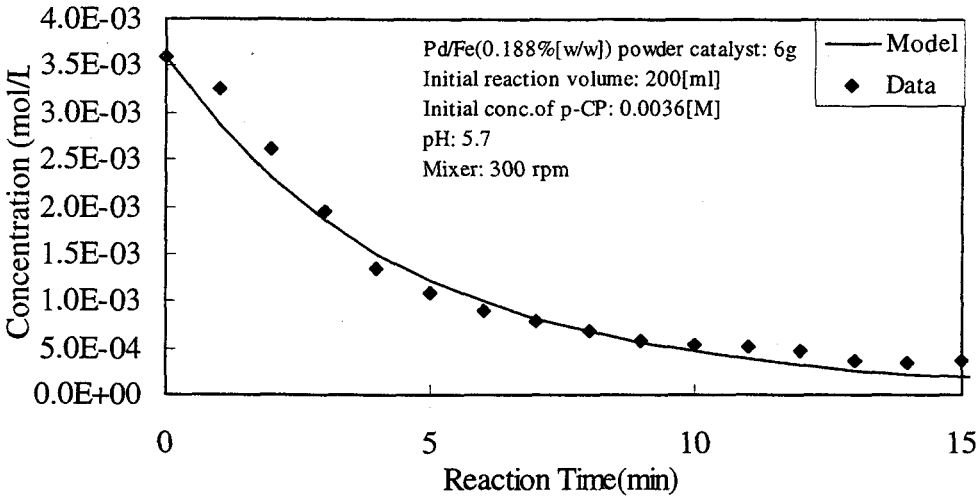

Figure 5.14 Comparison of p-chlorophenol concentration in dechlorination of p-chlorophenol with model output

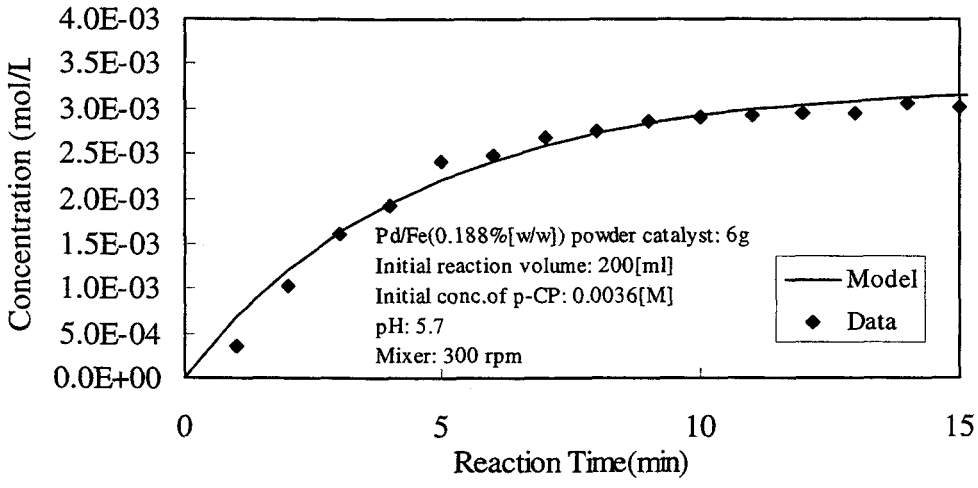

Figure 5.15 Comparison of phenol concentration in dechlorination of p-chlorophenol with model output

The reaction rate constants, k_1 to k_7, and deactivation rate constant, k_d, were determined by minimization of the objective function using IMSL optimization subroutine. All experimental data available are used in this optimization process. The results are represented in Table 5.1.

Table 5.1: Obtained values of rate constants and deactivation rate constant

Reaction Rate Constants	Units	Over All Optimized Values	Indepently Determined Values
k_1	$m^3/s\text{-}kg_{catalyst}$	0.0273	N/A
k_2	$m^3/s\text{-}kg_{catalyst}$	0.00381	N/A
k_3	$m^3/s\text{-}kg_{catalyst}$	0.0153	N/A
k_4	$m^3/s\text{-}kg_{catalyst}$	0.0239	N/A
k_5	$m^3/s\text{-}kg_{catalyst}$	0.0571	N/A
k_6	$m^3/s\text{-}kg_{catalyst}$	0.0606	0.19 (Graham, 1998)
k_7	$m^3/s\text{-}kg_{catalyst}$	0.0626	N/A
k_d	1/s	0.000205	0.000182 (Graham, 1998)

The values of all of the rate constants are of the order magnitude of 10^{-2} except for k_2 which is 10^{-3} . This represents that the dechlorination of 2,4,6-trichlorophenol to 2,4-dichlorophenol is the more preferred pathway than to 2,6-dichlorophenol. Furthermore, from dichlorophenol to monochlorophenol, k_5 which shows the rate of dechlorinating 2,6-dichlorophenol to o-chlorophenol is slightly larger than the summation of k_3 and k_4 which is the rate of dechlorinating 2,4-dichlorophenol to o-chlorophenol and p-chlorophenol. Dechlorination ratre of monochlorophenols (o-chlorophenol and p-chlorophenol) are almost of the same magnitude.

The effect of pH on the deactivation rate of dechlorination reaction on the powder Pd/Fe catalyst has been investigated (Graham, 1998). A correlation was obtained as shown in Equation 5.10.

$k_d = 0.091\ [H^+]$ [1/s] (5.10)

The value of deactivation rate constant calculated from this correlation at pH 5.7 is 1.82×10^{-4}. The value of k_d obtained from model fitted in this study agrees well with the value calculated from Equation 5.10.

.

5.2 Dechlorination of 2,4,6-trichlorophenol on Pd/Fe Catalyst in MSFB Entrapped in Alginate Beads

The experimental data for dechlorination of 2,4,6-trichlorophenol using Pd/Fe catalyst entrapped in alginate beads in MSFB were shown in section 4.2. The mathematical model which describes the change of the 2,4,6-trichlorophenol concentration due to the mass transfer from the bulk of the liquid to the surface of beads, diffusion through the alginate beads, the dechlorination reaction, and the deactivation on the entrapped Pd/Fe catalyst inside the beads was developed in section 2.3 and used to fit the experimental data.

$$\frac{\partial C_l(r,t)}{\partial t} = D_e\left(\frac{\partial^2 C_l(r,t)}{\partial r^2} + \frac{2}{r}\frac{\partial C_l(r,t)}{\partial r}\right) - \frac{k^*}{V'_{bd}(1-\phi)} C_l(r,t) a^n \qquad (2.19)$$

I.C.

Bead Liquid: $C_l(r, t=0) = C_{l,0}$ (2.22)

Bulk Liquid: $C_b(t=0) = C_{b,0}$ (2.23)

B.C.

r = 0, $$\left.\frac{\partial C_l(r,t)}{\partial r}\right|_{r=0} = 0 \qquad (2.24)$$

r = R $$D_e(1-\phi)\left.\frac{\partial C_l(r,t)}{\partial r}\right|_{r=R} = k_l\left[C_b(t) - C_l(R,t)\right] \qquad (2.20)$$

Mass balance of bulk liquid:

$$\frac{dC_b(t)}{dt} = -k_l\frac{3}{R}\frac{(1-\varepsilon)}{\varepsilon}\left[C_b(t) - C_l(R,t)\right] \qquad (2.21)$$

The model is solved by using a finite difference numerical method. Four parameters, k, k_d, De, and k_l, in this model were determined by an optimization subroutine. Figure 5.16 shows the results of the modeling applied to two independent experiments in the MSFB system. The value of the parameters obtained from the experiments are also shown in Table 5.2 and 5.3.

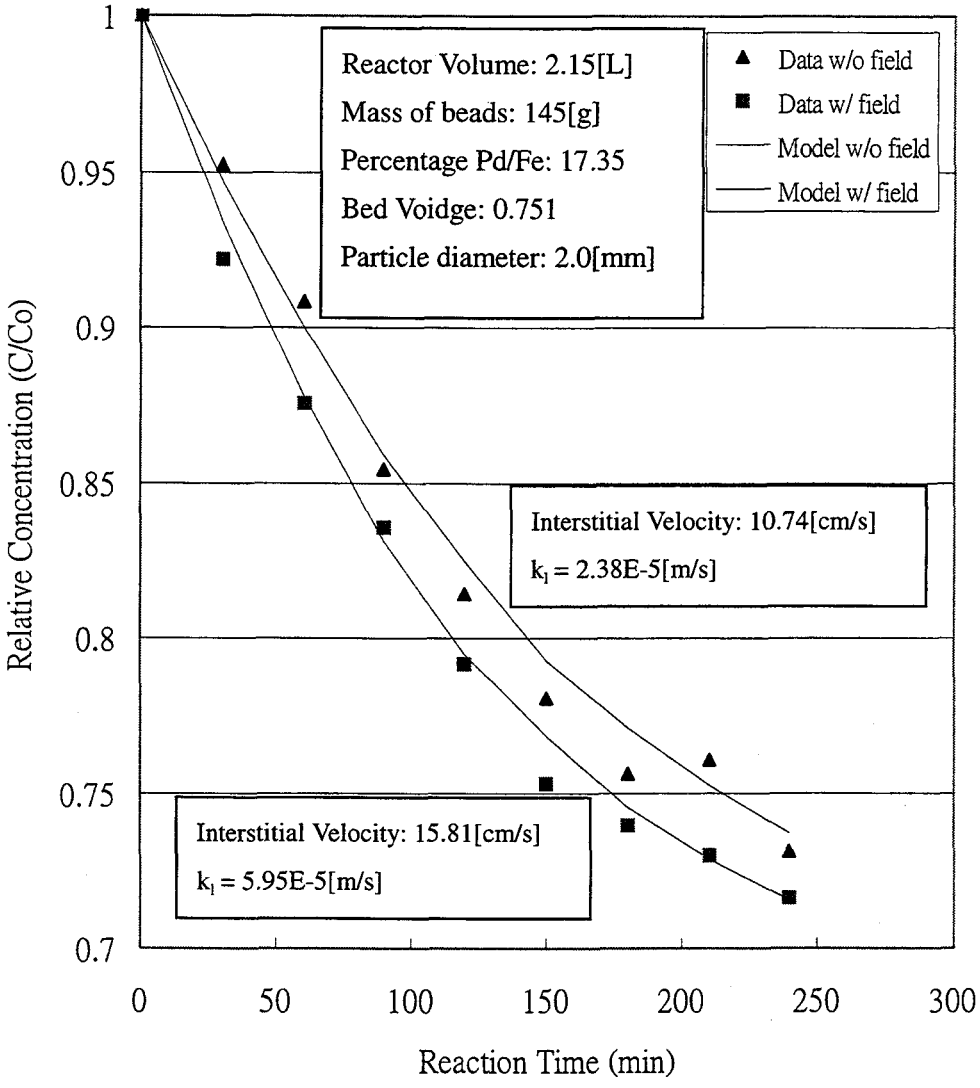

Figure 5.16 Applied dechlorination model for dechlorinationwithin Pd/Fe catalyst entrapped alginate beads in MSFB

Table 5.2: Comparison of Values Without an Applied Field

Parameter	Units	Optimized Values	Indepently Determined Values
k	$m^3/s\text{-}kg_{catalvst}$	$2.98x10^{-2}$	$3.11x10^{-2}$(Experiment)
k_d	1/s	$2.05x10^{-4}$	$2.05x10^{-4}$(Experiment) $1.82x10^{-4}$ (Graham,1998)
D_e	m^2/s	$1.83x10^{-11}$	$6.7x10^{-10}$ (Wilke-Chang, 1955)
k_l	m/s	$3.5x10^{-5}$	N/A

Table 5.3: Comparison of Values for an Applied Field

Parameter	Units	Optimized Values	Indepently Determined Values
k	$m^3/s\text{-}kg_{catalvst}$	$3.16x10^{-2}$	$3.11x10^{-2}$(Experiment)
k_d	1/s	$2.91x10^{-4}$	$2.05x10^{-4}$(Experiment) $1.82x10^{-4}$ (Graham,1998)
D_e	m^2/s	$2.68x10^{-11}$	$6.7x10^{-10}$ (Wilke-Chang, 1955)
k_l	m/s	$4.73x10^{-5}$	N/A

The value of the reaction rate constant, k, obtained from the model agrees well with the value obtained from the experimental result of dechlorination on the powder Pd/Fe catalyst. Also, the value for deactivation rate constant shows good agreement. The result for the mass transfer coefficient shows the expected enhancement of about 35% above the value obtained in ordinary fluidized bed when the magnetic field is applied.

The diffusion coefficient, however, is of the magnitude of 10^{-11}. The diffusion coefficient in water for 2,4,6-trichlorophenol obtained by Wilke-Chang equation is 6.7×10^{-10}[m^2/s] (Appendix H). One possible explanation for this small diffusion coefficient value is the presence of surfactant. Surfactant in aqueous solution can form micelles, which are macromolecules having hydrophobic interiors and hydrophilic exteriors. The affinity of the 2,4,6-trichlorophenol for the hydrophobic interior of micelles can increase the solubility in water, but the diffusivity is reduced because of the large molecule size. No experimental data are published for this or similar system and no correlation is reported that can predict the diffusion coefficient for this or similar system.

CHAPTER 6

CONCLUSIONS AND RECOMMENDATIONS

6.1 Conclusions

In this work, we investigated the chemical kinetics of the dechlorination of 2,4,6-trichlorophenol on the Pd/Fe catalyst. Four experiments, dechlorination of 2,4,6-trichlorophenol, 2,4-dichlorophenol, 2,6-dichlorophenol, and p-chlorophenol were performed in a batch reactor. All factors that can effect the reaction kinetics including system pH, Pd/Fe interfacial area, and Pd/chlorine removal were maintained constant during experiment.

The pseudo-first order rate kinetics with respect to the chlorinated hydrocarbon concentration is found to be the most appropriate for modeling purpose.

$$-\frac{d(VC_A)}{dt} = (kW)C_A a = k^* C_A a \qquad (2.11)$$

$$-\frac{da}{dt} = k_d a^n \qquad (2.12)$$

The possible pathway for dechlorinating 2,4,6-trichlorophenol to phenol was proposed.

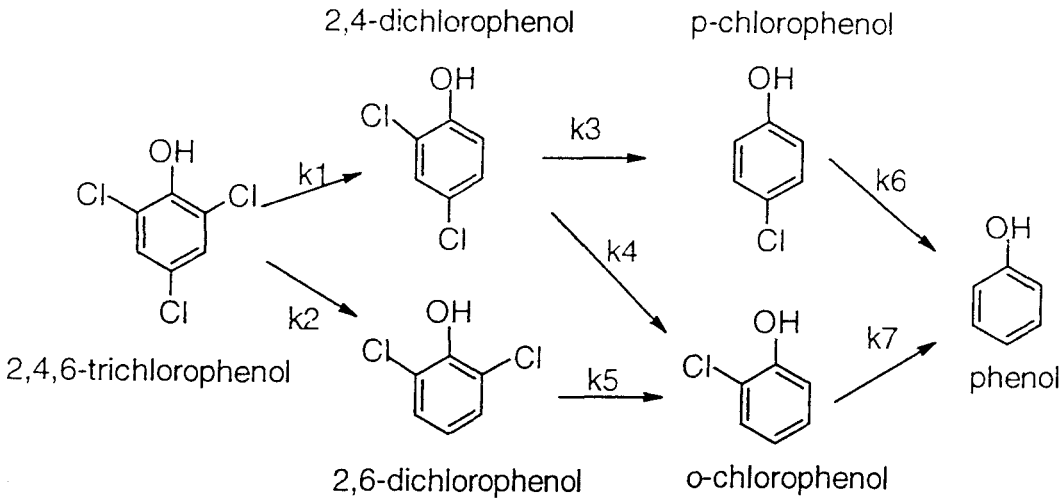

Figure 2.3 Illustration of dechlorination of 2,4,6-trichlorophenol on Pd/Fe catalyst

The rate equations for all compounds involved in this reaction were developed as follows:

$$-\frac{d(VC_1)}{dt} = (k_1^* + k_2^*)C_1 a \tag{2.13}$$

$$-\frac{d(VC_2)}{dt} = (k_3^* + k_4^*)C_2 a - k_1^* C_1 a \tag{2.14}$$

$$-\frac{d(VC_3)}{dt} = k_5^* C_3 a - k_2^* C_1 a \tag{2.15}$$

$$-\frac{d(VC_4)}{dt} = k_6^* C_4 a - k_3^* C_2 a \tag{2.16}$$

$$-\frac{d(VC_5)}{dt} = k_7{}^{*}C_5 a - k_4{}^{*}C_2 a - k_5{}^{*}C_3 a \qquad (2.17)$$

$$-\frac{d(VC_6)}{dt} = -k_6{}^{*}C_6 a - k_7{}^{*}C_5 a \qquad (2.18)$$

initial condition for these differential equations are:

at $t=0$,

$$C_1 = C_{1,0} \qquad (2.19)$$

$$C_2 = C_3 = C_4 = C_5 = C_6 = 0 \qquad (2.10)$$

These rate equations were solved numerically and fitted to all the experimental data to determine the reaction rate constants and deactivation rate constant. The result is shown as follows:

Table 5.1: Value of rate constants and deactivation rate constant from optimization subroutine

Reaction Rate Constants	Units	Over All Optimized Values	Indepently Determined Values
k_1	$m^3/s\text{-}kg_{catalyst}$	0.0273	N/A
k_2	$m^3/s\text{-}kg_{catalyst}$	0.00381	N/A
k_3	$m^3/s\text{-}kg_{catalyst}$	0.0153	N/A
k_4	$m^3/s\text{-}kg_{catalyst}$	0.0239	N/A
k_5	$m^3/s\text{-}kg_{catalyst}$	0.0571	N/A
k_6	$m^3/s\text{-}kg_{catalyst}$	0.0606	0.19 (Graham, 1998)
k_7	$m^3/s\text{-}kg_{catalyst}$	0.0626	N/A
k_d	1/s	0.000205	0.000182 (Graham, 1998)

The second object in this work was to investigate the mass transfer phenomena in the application of the Pd/Fe catalyst for remediation of contaminated liquids in MSFB. Two experiments were performed in the MSFB. The mathematical model for this reactor system was developed in section 2.3 and was solved by using finite difference method.

$$\frac{\partial C_l(r,t)}{\partial t} = D_e\left(\frac{\partial^2 C_l(r,t)}{\partial r^2} + \frac{2}{r}\frac{\partial C_l(r,t)}{\partial r}\right) - \frac{k^*}{V}C_l(r,t)a^n \tag{2.19}$$

I.C.

Bead Liquid: $C_l(r,t=0) = C_{l,0}$ (2.22)

Bulk Liquid: $C_b(t=0) = C_{b,0}$ (2.23)

B.C.

r = 0, $\left.\frac{\partial C_l(r,t)}{\partial r}\right|_{r=0} = 0$ (2.24)

r = R, $D_e(1-\phi)\frac{\partial C_l(R,t)}{\partial r} = k_l[C_b(t) - C_l(R,t)]$ (2.20)

Mass balance for bulk liquid:

$$\frac{dC_b(t)}{dt} = -k_l\frac{3}{R}\frac{(1-\varepsilon)}{\varepsilon}[C_b(t) - C_l(R,t)] \tag{2.21}$$

Four parameters, reaction rate constant k for dechlorination of 2,4,6-trichlorophenol, deactivation rate constant k_d, diffusion coefficient De, and mass transfer coefficient k_l were determined through the optimization process. The results are shown in below:

Table 5.1: Comparison of Values Without an Applied Field

Parameter	Units	Optimized Values	Indepently Determined Values
k	$m^3/s\text{-}kg_{catalyst}$	$2.98x10^{-2}$	$3.11x10^{-2}$(Experiment)
k_d	1/s	$2.05x10^{-4}$	$2.05x10^{-4}$(Experiment) $1.82x10^{-4}$ (Graham,1998)
D_e	m^2/s	$1.83x10^{-11}$	$6.7x10^{-10}$ (Wilke-Chang, 1955)
k_l	m/s	$3.5x10^{-5}$	N/A

Table 5.2: Comparison of Values for an Applied Field

Parameter	Units	Optimized Values	Indepently Determined Values
k	$m^3/s\text{-}kg_{catalyst}$	$3.16x10^{-2}$	$3.11x10^{-2}$(Experiment)
k_d	1/s	$2.91x10^{-4}$	$2.05x10^{-4}$(Experiment) $1.82x10^{-4}$ (Graham,1998)
D_e	m^2/s	$2.68x10^{-11}$	$6.7x10^{-10}$ (Wilke-Chang, 1955)
k_l	m/s	$4.73x10^{-5}$	N/A

6.2 Recommendations

This study explored the kinetics of dechlorination of 2,4,6-trichlorophenol on Pd/Fe catalyst. Other multichlorinated phenol such as pentachlorophenol(PCP) or PCBs can be further investigated in the similar manner. The results of this study can be incorporated in the further studies.

Moreover, the effect of the presence of surfactant on diffusion coefficient and/or reaction rate constants can be further studied. Different surfactant or different ratio of surfactant to water in solution can be used. Baohua Gu indicated that the presence of surfactant and cosolvent will reduce the degradation rate of PCB by Pd/Fe catalyst(Baohua Gu, 1997).

REFERENCES

Abdul, A.S., and Glbson, T.L.(1991) Laboratory Studies of Surfactant-Enhanced Washing of Polychlorinated Biphenol from Sandy Material. *Environ.Sci. Technol.*, 25, 665-671.

Abdul, A.S., Glbson, T.L., and Rai, D.N.(1990) Selection of Surfactant for the Removal of Petroleum Products from Shallow Sandy Aquifers. *Ground Water.* Vol. 28, No. 6, 920-926.

Abdul, A.S., Glbson, T.L., Ang, C.C., Smith, J.C., and Sobczynski, R.E.(1992) In Situ Surfactant Washing of Polychlorinated Biphenol and Oils from a Contaminated Site. *Ground Water.*Vol. 30. No. 2. 219-231.

Al-Mulhim, M. (1995) Enhancement of Mass Transfer Coefficient in a Magnetically Stabilized Liquid-Solid Fluidized Bed, M. S. Thesis, Oregon State University (1995).

Bae, H. S., Lee, James M., and Lee, S. T.(1997) Biodegradation of the Mixture of 2,4,6-ttrichlorophenol, 4-chlorophenol, and Phenol by a Defined Mixed Culture. *J. Gen. Appl. Microbiol.*, 43, 97-103.

Cheng, I. F., Fernando, Q., and Korte, N. (1997) Electrochemical Dechlorination of 4-Chlorophenol to Phenol. *Environ. Sci. Technol.,* **31** (4), 1074-1078.

Federal Register. 1987. Notice of the First Priority List of Hazardous Susbstances That Will be the Subject of Toxicological Profiles. *Fed. Regist.* 52:12866-12874.

Giordano, F.R., and Weir, M.D. (1991) *Differential Equations A Modeling Approach*, Addison-Wesley Publishing Company.

Graham, L. J(1998) Dechlorination of *p*-Chlorophenol on Bimetallic Pd/Fe Catalyst in a Magnetically Stabilized Fluidized Bed; Experiment and Theory. Ph.D. Thesis, Oregon
State University (1998).

Graham, L. J. and Jovanovic G. (1998) Dechlorination of p-Chlorophenol on a Pd/Fe Catalyst in a Magnetically Stabilized Fluidized Bed; Implications for Sludge and Liquid Remediation, *ISCRE Conference*, Los Angeles, CA.

Grittini C, Malcomsen, M., Fernando, Q., and Korte, N (1995) Rapid Dechlorination of Polychlorinated Biphenyls on the Surface of a Pd/Fe Bimetallic System, *Environ. Sci. and Technol.*, **29** (11), 2898-2900.

Gu, B., Liang, L., Cameron, P., West, O., and Korte, N. (1997) Degradation of Trichloroethylene (TCE) and Polychlorinated Biphenyl (PCB) by Fe and Fe-Pd Bimetals in the Presence of a Surfactant and a Cosolvent, *Proceedings of the 1997 International Containment Technology Conference and Exhibition*, St. Petersburg, FL.

Juteau, P., Beaudet, R., McSween, G.,Lepine, F., and Bisaillon, J.G.(1995) Study of the Reductive Dechlorination of Pentachlorophenol by a Methanogenic Consortinm, *Microbiol.* 41:862-868.

Levenspiel, O. (1996) *The Chemical Reactor Omnibook.*, Oregon State University Book Stores, OR..

Liu, Y, Schwartz, J., and Cavallaro, C. L. (1995) Catalytic Dechlorination of Polychlorinated Biphenyls. *Environ. Sci. Technol.*, **29** (3), 836-840.

Liu, S. M.,Kuo,C. E., and Hsu,T. B.(1996) Reductive Dechlorination of Chlorophenols and Pentachlorophenol in Anoxic Estuarine Sediments,*Chemosphere*,Vol.32, No 7, pp. 1287-1300.

McCann, M., Boersma, P., Danko, J. and Guerriero, M. (1994) Remediation of a VOC-Contaminated Superfund Site Using Soil Vapor Extraction, Groundwater Extraction, and Treatment: A Case Study. *Environmental Progress.* **13** (3), 209-213.

Muftikian, R., Fernando, Q., and Korte, N. (1995) A Method for the Rapid Dechlorination of Low Molecular Weight Chlorinated Hydrocarbons in Water, *Wat. Res.*, **29** (10), 2434-2439.

Passivirta, J., Knuutinen, J., Maatela, P., Paukku, R.,Soikkeli, J., and Sarkka, J.(1988) *Chemosphere*,17, 137-146.

Shishido, M. and Toda, M. (1996) Simulation of Oxygen Concentration Profile in Calcium Alginate Gel Beads Entrapping Microbes During Biological Phenol Degradation, *Chemical Engineering Science*, **51** (6)

Suntio,L.R., Shiu, W.Y. and Mackay, D.(1988). *Chemosphere*, 17, 11249-1290.

Welty, J.R., Wicks, C.E., and Wilson, R.E.(1984) *Fundamentals of Momentum, Heat, and Mass Transfer 3rd Ed.* John Wiley and Sons, NY

APPENDICES

APPENDIX A

DERIVATION OF DECHLORINATION OF 2,4,6-TRICHLOROPHENOL IN ALGINATE BEADS WITH ENTRAPPED Pd/Fe CATALYST MODEL

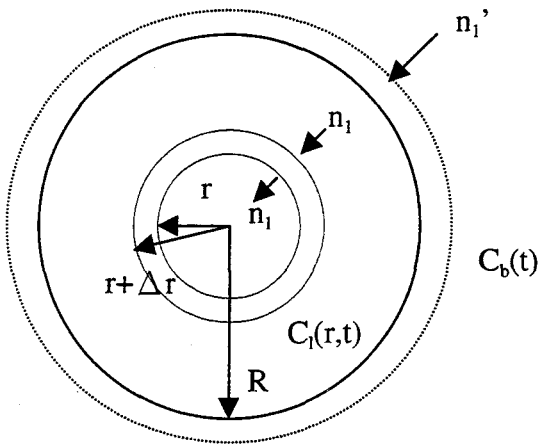

A differential mass balance of any compound within the liquid phase in the alginate bead is given by:

$$V_{gl}\left(C_l(r,t)\Big|_{t+\Delta t} - C_l(r,t)\Big|_t \right) = n_1 \Delta t A_{gl}\Big|_{r+\Delta r} - n_1 \Delta t A_{gl}\Big|_r - V_{gl}\frac{k^*}{V_{gl}} C_l(r,t) a^n \Delta t \qquad \text{(A.1)}$$

where,

$$n_1 = De\frac{\partial C_l(r,t)}{\partial r} \qquad \text{(A.2)}$$

$$V_{gl} = V_{bd}(1-\phi) = 4\pi r^2 \Delta r(1-\phi) \tag{A.3}$$

$$A_{gl} = A_{bd}(1-\phi) = 4\pi r^2(1-\phi) \tag{A.4}$$

Insert Equation A.2, A.3, and A.4 into Equation A.1, the final differential equation can be obtained shown as Equation A.5

$$\frac{\partial C_l(r,t)}{\partial t} = D_e\left(\frac{\partial^2 C_l(r,t)}{\partial r^2} + \frac{2}{r}\frac{\partial C_l(r,t)}{\partial r}\right) - \frac{k^*}{V_{gl}} C_l(r,t) a^n \tag{A.5}$$

The initial conditions of the bulk and bead liquid as well as the boundary condition for the center of the bead respectively are:

Bead Liquid: $C_l(r, t=0) = C_{l,0}$ (A.6)

Bulk Liquid: $C_b(t=0) = C_{b,0}$ (A.7)

At the center of the bead at all times: $\left.\frac{\partial C_l(r,t)}{\partial r}\right|_{r=0} = 0$ (A.8)

Assume there is no reaction and accumulation on boundary. The boundary condition at $r = R$ for the alginate bead is obtained from:

Mass diffused into beads = mass transferred from thin film, which can be represents

as:

$$n_1 A_{gl} = n'_1 A_{bd} \tag{A.9}$$

where

$$n_1 = De \left.\frac{\partial C_l(r,t)}{\partial r}\right|_{r=R} \tag{A.10}$$

$$n'_1 = k_l[C_b(t) - C_l(r,t)] \tag{A.11}$$

$$A_{gl} = A_{bd}(1-\phi) \tag{A.12}$$

Insert Equation A.10, A.11, and A.12 into Equation A.9, the boundary condition at r = R can be expressed as:

$$D_e(1-\phi)\frac{\partial C_l(R,t)}{\partial r} = k_l[C_b(t) - C_l(R,t)] \tag{A.13}$$

A mass balance on the bulk liquid concentration, $C_b(t)$, is related to the diffusion at the outer boundary and is given by:

$$-V_{bl}\frac{dC_b(t)}{dt} = A_{bd}k_l[C_b(t) - C_l(R,t)] \tag{A.14}$$

where

$$V_{bd} = \varepsilon V_r \tag{A.15}$$

$$A_{bd} = 4\pi R^2 \tag{A.16}$$

$$V_{bd} = \frac{4}{3}\pi R^3 \tag{A.17}$$

$$A_{bd} = \frac{3}{R}V_{bd} = \frac{3(1-\varepsilon)}{R}V_r \tag{A.18}$$

Insert Equation A.15 and A.18 into Equation A.14, the mass balance on the bulk liquid concentration can be obtained as:

$$\frac{dC_b(t)}{dt} = -k_l \frac{3}{R}\frac{(1-\varepsilon)}{\varepsilon}\left[C_b(t) - C_l(R,t)\right] \tag{A.18}$$

APPENDIX B

HPLC ANALYSIS:

STANDARD CURVES FOR ALL CHLOROPHENOLS AND PHENOL

Standard curves for absorbance vs concentration were determined for 2,4,6-trichlorophenol, 2,4-dichlorophenol, 2,6-dichlorophenol, o-chlorophenol, p-chlorophenol and phenol. A series of solutions with know concentrations of 2,4,6-trichlorophenol, 2,4-dichlorophenol, 2,6-dichlorophenol, o-chlorophenol, p-chlorophenol and phenol were prepared in 1%[w/w] surfactant water solution and thoroughly mixed. These solutions were individually injected into the HPLC column. Mobile phase which consists of 70[%] acetic-acid methanol solution(1% acetic-acid, 99% HPLC grade methanol) and 30[%] acetic-acid deionized water solution(1% acetic-acid, 99% deionized water) is used for determining the concentration of 2,4,6-trichlorophenol and 2,4-dichlorophenol and which consists of 55[%] acetic-acid methanol solution(1% acetic-acid, 99% HPLC grade methanol) and 45[%] acetic-acid deionized water solution(1% acetic-acid, 99% deionized water) is used for determining the concentration of 2,6-dichlorophenol, 4-chlorophenol, 2-chlorophenol, and phenol. Their respective absorbances were recorded by Visual Designer software. The solution concentration vs. peak area of the absorbance readings were plotted from Figures B.1 to B.6, respectively for use in determining reaction concentrations.

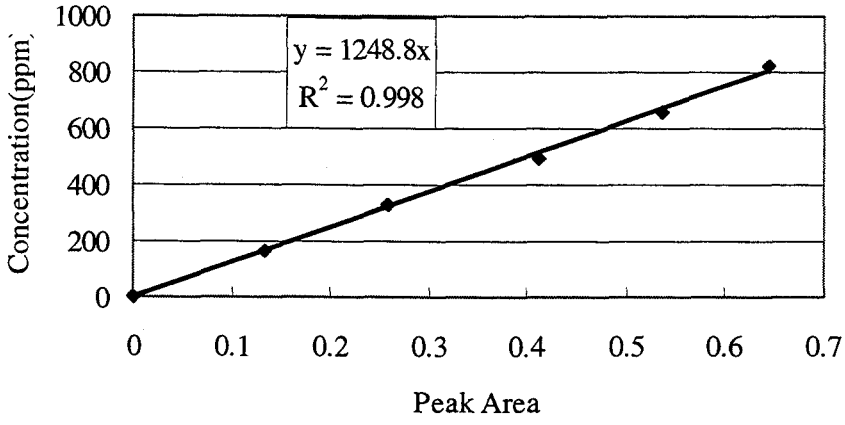

Figure B.1: Standard curve for HPLC analysis of 2,4,6-TCP concentration

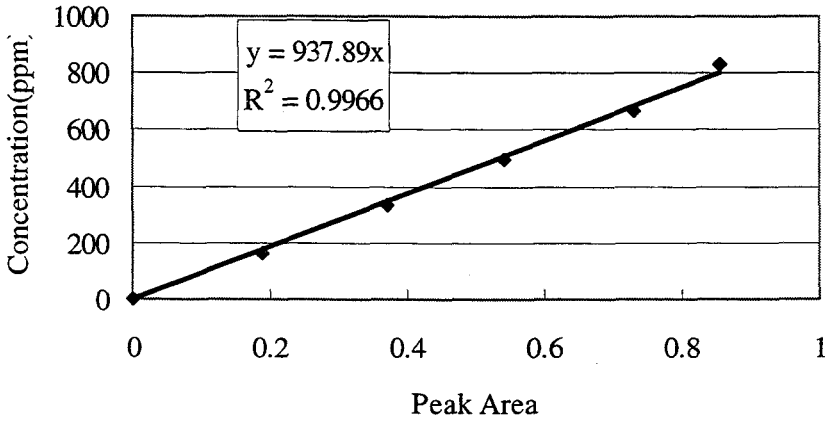

Figure B.2: Standard curve for HPLC analysis of 2,4-DCP concentration

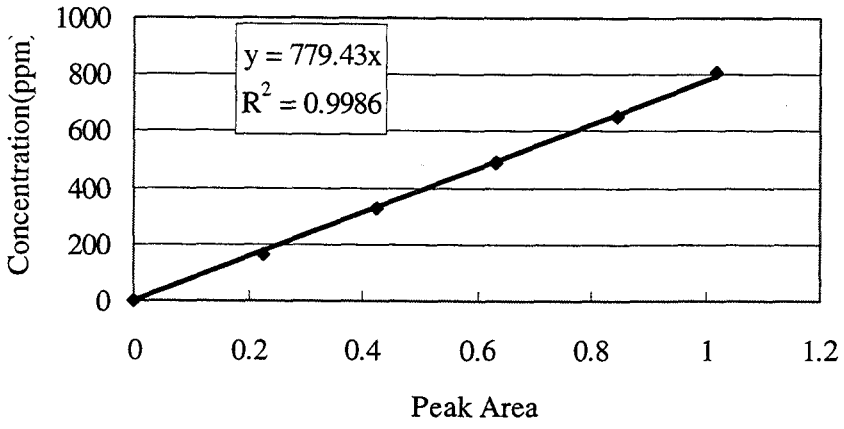

Figure B.3: Standard curve for HPLC analysis of 2,6-DCP concentration

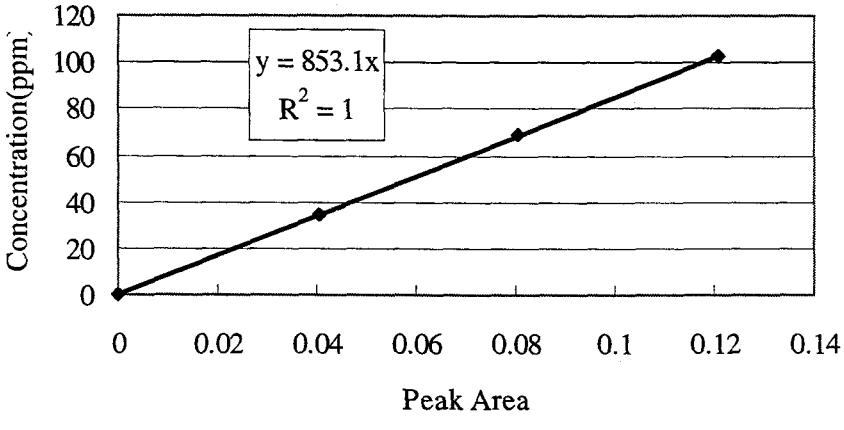

Figure B.4: Standard curve for HPLC analysis of p-chlorophenol concentration

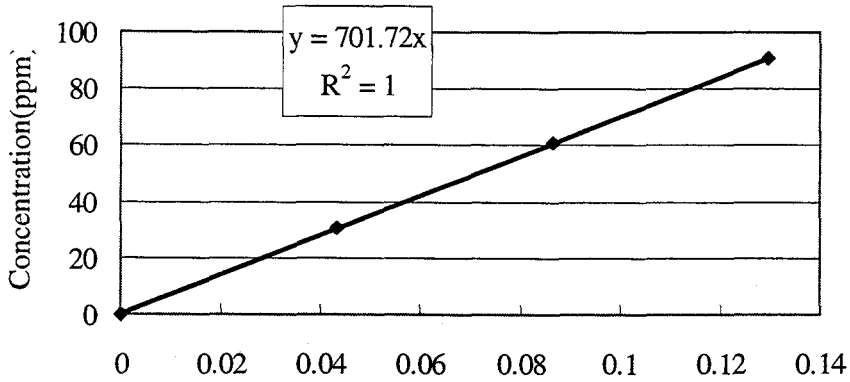

Figure B.5: Standard curve for HPLC analysis of o-chlorophenol concentration

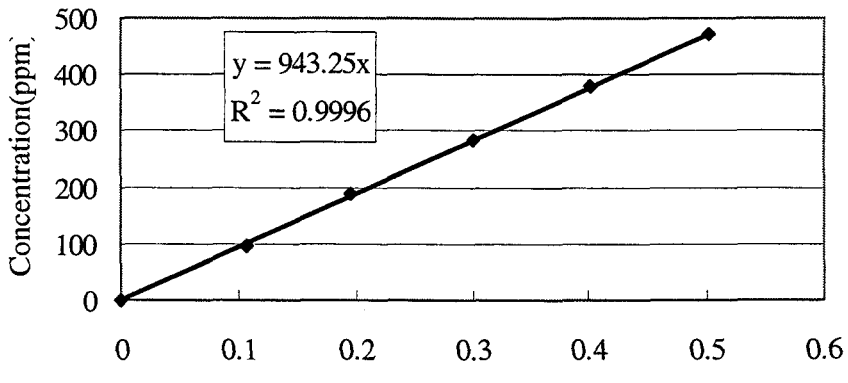

Figure B.6: Standard curve for HPLC analysis of phenol concentration

APPENDIX C

ALGINATE BEAD PRODUCTION PROCEDURE

The particles used in this study are composite particles consisting of sodium alginate and Pd/Fe catalyst powder. The following instructions detail the preparation of the 1.5 [w/w %] sodium alginate solution mixed with Pd/Fe catalyst used to produce alginate gel beads. The properties of the alginate and Pd/Fe powder are given in Table C-1.

1. Weigh 394.0 [g] of deionized water into a 600 [ml] beaker.

2. Weigh 6.0 [g] of Keltone HV sodium alginate into a weighing cup.

3. As deionized water is mixed, slowly add alginate powder to the 600 [ml] beaker.

4. Mix the solution for at least one hour to ensure a homogeneous solution. The mixer speed should be increased as the viscosity of the solution increases.

5. As the solution continues to mix, add 84 [g] of the freshly prepared Pd/Fe catalyst.

6. Mix for 60 minutes to evenly distribute the Pd/Fe catalyst within the alginate solution.

Table C-1: Alginate and Pd/Fe Properties

Material	Powder [μm]	Size	Density [kg/m^3]
Alginate (Keltone HV)	1.8		1.59
Pd/Fe	5-8		7.87

This solution is poured into a pressurized vessel and extruded into a calcium chloride solution. Air supplied to the tip of the nozzle and the amount of pressurization of the vessel allows for control of bead size.

The alginate bead is released into $CaCl_2$ solution where the alginate exchanges two Na^+ ions for a Ca^{2+} which immediately creates the protective "skin" of the particle. To ensure reproducible gel beads, the particles are left in a 1.0 [M] $CaCl_2$ solution for exactly 60 minutes to maintain a consistent extent of polymerization. The reaction between calcium ions and the alginate molecules is represented by the following (Kelco Company, 1998):

$$2Na(Alg)+Ca^{2+} \leftrightarrow \quad 2Ca(Alg)_2 + 2Na^+ \qquad (C.1)$$

APPENDIX D

MSFB FLOWRATE CALIBRATION AND FIELD GRADIENT

To determine the flowrate within the MSFB for experimental work, a series of measurements were taken which measured the volume of water pumped through the MSFB over a period of time vs. the pressure drop given by the flow. Figure D.1 gives the plotted values. A linear portion of the curve over the range of flowrates used during experimental work can be seen in Figure D.2.

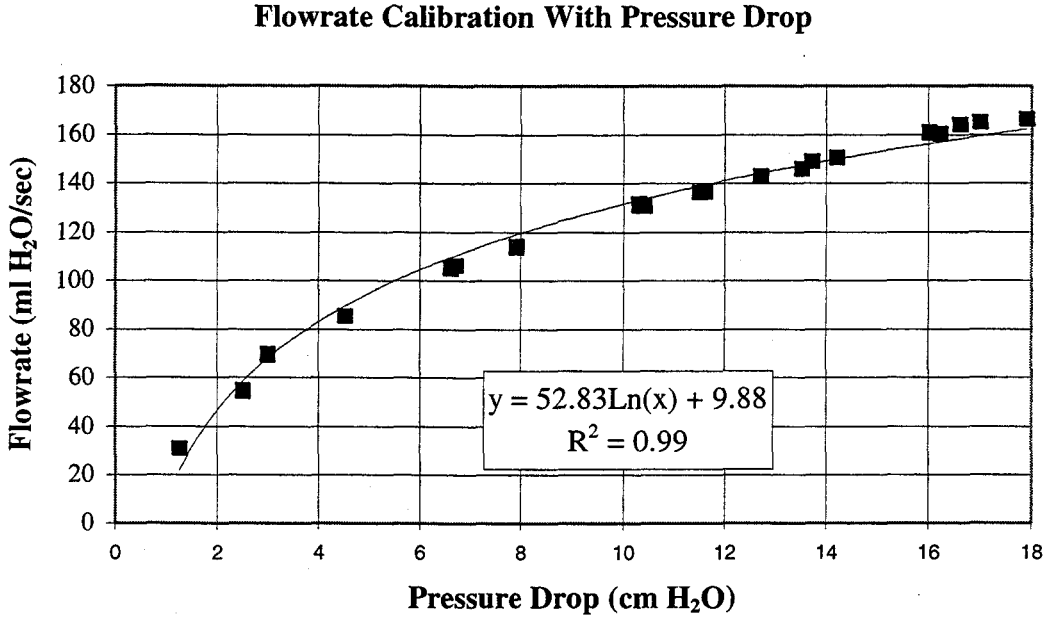

Figure D.1: Calibration curve for MSFB flowrate determination over full pumping range.

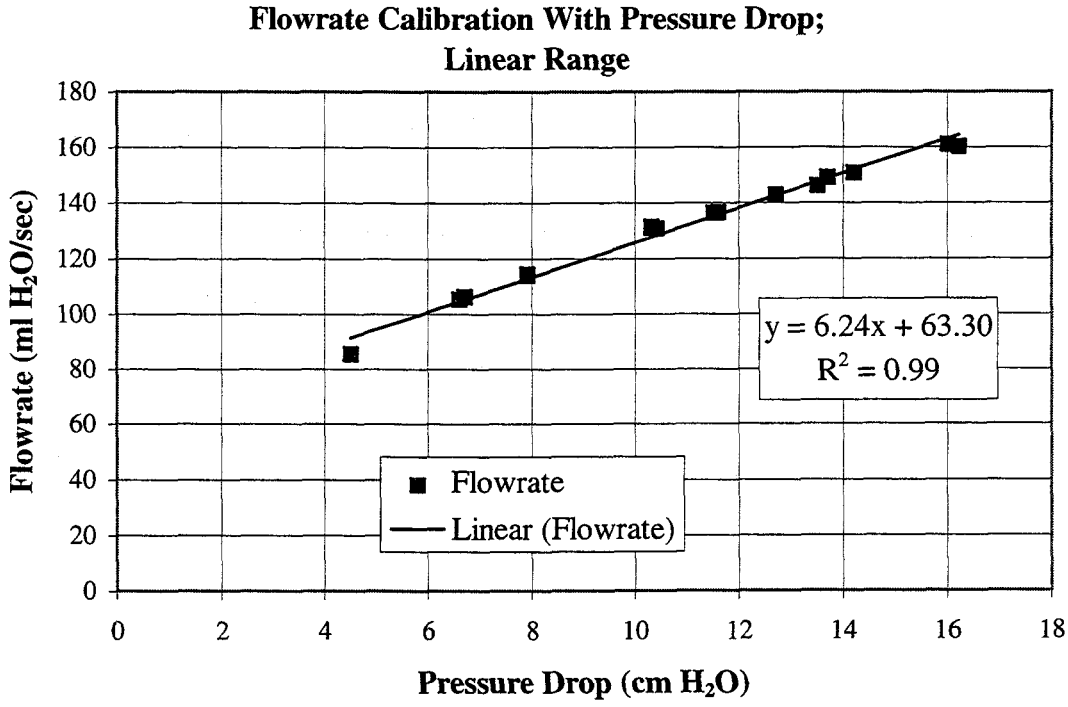

Figure D.2: Linear portion of calibration curve for flowrate determination in the MSFB.

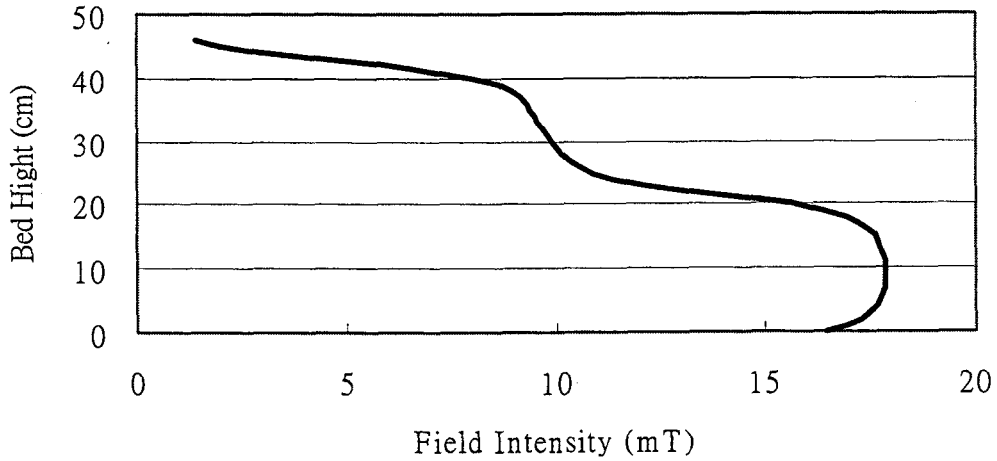

Figure D.3: MSFB applied magnetic field gradient.

APPENDIX E

NUMERICAL SOLUTION FOR THE PARTIAL DIFFERENTIAL EQUATION FOR DECHLORINATION OF 2,4,6-TRICHLOROPHENOL ON ALGINATE BEAD ENTRAPPED Pd/Fe CATALYST

Numerical approximation of the partial differential equations for 2,4,6-trichlorophenol diffusion through alginate beads with entraped Pd/Fe catalyst and the respective boundary conditions is described below.

Bead Diffusion With Reaction Including External Mass Transfer Resistance
(Chapter 2: Equations 2.21-2.26)

Equation 2.21: $$\frac{\partial C_l(r,t)}{\partial t} = D_e\left(\frac{\partial^2 C_l(r,t)}{\partial r^2} + \frac{2}{r}\frac{\partial C_l(r,t)}{\partial r}\right) - \frac{k^*}{V}C_l(r,t)a^n$$

$$C_l(I,J+1) = C_l(I,J) + (D_e * \Delta t)\left[\left(\frac{C_l(I+1,J) - 2*C_l(I,J) + C_l(I-1,J)}{\Delta r^2}\right)\right] +$$

$$(D_e * \Delta t)\frac{2}{R} * \left(\frac{C_l(I+1,J) - C_l(I,J)}{\Delta r}\right) - \left(\frac{k^* a \Delta t}{V}\right)\left(\frac{C_l(I+1,J) + C_l(I,J)}{2}\right) \qquad \text{(E.1)}$$

with $a = exp^{-k_d t}$

Equation 2.25: $$D_e(1-\phi)\frac{\partial C_l(R,t)}{\partial r} = k_l[C_b(t) - C_l(R,t)]$$

$$C_l(R+1,J) = C_l(R,J) + \frac{k_l \Delta r}{D_e(1-\phi)}\left(C_b(J) - C_l(R,J)\right) \qquad \text{(E.2)}$$

Equation 2.26: $\dfrac{dC_b(t)}{dt} = -k_l \dfrac{3}{R}\dfrac{(1-\varepsilon)}{\varepsilon}\left[C_b(t) - C_l(R,t)\right]$

$$C_b(J+1) = C_b(J) - k_l \Delta t \frac{3}{R}\frac{(1-\varepsilon)}{\varepsilon}\left(C_b(J) - C_l(R,J)\right) \qquad \text{(E.3)}$$

Equation 2.24: $\left.\dfrac{\partial C_l(r,t)}{\partial r}\right|_{r=0} = \textit{finite}$

$$C_l(I,J) = C_l(I+1,J) \qquad \text{(E.4)}$$

APPENDIX F

FORTRAN PROGRAM FOR SOLVING REACTION RATE CONSTANTS AND DEACTIVATION RATE CONSTANT

```
C  ksdths.for
c
c  data from exp15,exp16,exp17, and exp21
c  find k1,k2,k3,k4,k5,k6,k7,kd
c
C
C                              DECLARATION OF VARIABLES

      INTEGER N,M,J
      PARAMETER (N=8)
C
      INTEGER I, MAXFN, NOUT
      REAL  DFPRED, FVALUE, G(N), GRADTL, X(N),XGUESS(N), XS(N)
      real C16(21,4),CMD16(1201,4),V1,V2,V3,V4,V5,V6,V7,V8,V9,V10,
     +     C17(21,3),CMD17(1201,3),U1,U2,U3,U4,U5,U6,U7,U8,U9,U10,
     +     C15(21,6),CMD15(1201,6),Y1,Y2,Y3,Y4,Y5,Y6,Y7,Y8,Y9,Y10,
     +     C21(21,2),CMD21(1201,2),Z1,Z2,Z3,Z4,Z5,Z6,Z7,Z8,Z9,Z10
     +     ,TIME(21)
      common CMD16,CMD17,CMD15,CMD21
      EXTERNAL ROSBRK, UMACH, UMCGF
C
      DATA XGUESS/0.05,0.005,0.05,0.05,
     +     0.05,0.05,0.05,0.05/
     +     ,XS/8*1.0E0/

C
      DFPRED = 0.0000001
      GRADTL = 5.E-12
```

```
      MAXFN = 0

C                          MINIMIZE THE ROSBRK FUNCTION

      CALL UMCGF (ROSBRK, N, XGUESS, XS, GRADTL,MAXFN, DFPRED,
     + X, G, FVALUE)
C                          PRINT THE VALUE

      CALL UMACH (2, NOUT)
      WRITE (NOUT,99999) (X(I), I=1, N), FVALUE, (G(I),I=1,N)
99999  FORMAT ('SOL:', 8(1x,E8.3), //,'THE FUNCTION '
     + 'EVALUATED AT THE SOLUTION IS ',2X,E10.3,//,
     + 'GRAD:',8(1x,E9.3),/)
C

      open(unit=5,file='15ksd.dat',status='new')
      do 150 K=1,16
      write(5,99)(CMD15((K-1)*20+1,1),CMD15((K-1)*20+1,2)
     +           ,CMD15((K-1)*20+1,3),CMD15((K-1)*20+1,4)
     +           ,CMD15((K-1)*20+1,5),CMD15((K-1)*20+1,6))
99     format(2x,F10.9,2x,F10.9,2x,F10.9,2x,F10.9,2x,F10.9,2x,F10.9)
150    continue
      close(unit=5)



      open(unit=6,file='16ksd.dat',status='new')
      do 250 K=1,16
      write(6,999)(CMD16((K-1)*20+1,1),CMD16((K-1)*20+1,2),
     +           CMD16((K-1)*20+1,3),CMD16((K-1)*20+1,4))
999    format(3x,F10.9,3x,F10.9,3x,F10.9,3x,F10.9)
250    continue
      close(unit=6)
```

```
      open(unit=7,file='17ksd.dat',status='new')
      do 350 K=1,16
      write(7,9999)(CMD17((K-1)*20+1,1),CMD17((K-1)*20+1,2)
     +            ,CMD17((K-1)*20+1,3))
9999   format(3x,F10.9,3x,F10.9,3x,F10.9)
350    continue
      close(unit=7)

      open(unit=8,file='21ksd.dat',status='new')
      do 450 K=1,16
      write(8,66)(CMD21((K-1)*20+1,1),CMD21((K-1)*20+1,2))
66     format(3x,F10.9,3x,F10.9)
450    continue
      close(unit=8)

      END
C     ================================================================
      SUBROUTINE ROSBRK (N, X, F)
      INTEGER N

      REAL X(N), F
C
      INTEGER K

      REAL C16(21,4),V1,V2,V3,V4,V5,V6,V7,V8,V9,V10,CMD16(1201,4),
     +     C17(21,3),U1,U2,U3,U4,U5,U6,U7,U8,U9,U10,CMD17(1201,3),
     +     C15(21,6),Y1,Y2,Y3,Y4,Y5,Y6,Y7,Y8,Y9,Y10,CMD15(1201,6),
     +     C21(21,2),Z1,Z2,Z3,Z4,Z5,Z6,Z7,Z8,Z9,Z10,CMD21(1201,2)
     +     ,E,dT
      common CMD16,CMD17,CMD15,CMD21

      CALL DATA(TIME,V1,V2,V3,V4,V5,V6,V7,V8,V9,V10,
     +             U1,U2,U3,U4,U5,U6,U7,U8,U9,U10,
     +             Y1,Y2,Y3,Y4,Y5,Y6,Y7,Y8,Y9,Y10,
```

```
     +               Z1,Z2,Z3,Z4,Z5,Z6,Z7,Z8,Z9,Z10)
        dT=0.05


        open (unit=5,file='exp21.dat',status='old')
        read (5,*)((C21(i,j),j=1,2),i=1,21)
        close (unit=5)

        CMD21(1,2)=C21(1,2)
        CMD21(1,1)=0.0

        do 40 I=1,300
        CMD21(I+1,2)=CMD21(I,2)+dT/((Z4*((I-1)*dT)**3+
     +                          Z3*((I-1)*dT)**2+
     +                          Z2*(I-1)*dT+Z1)/1000)*
     +             (-X(6)*CMD21(I,2)*EXP(-X(8)*(I-1)*dT)
     +             -CMD21(I,2)*((3*Z4*((I-1)*dT)**2+2*Z3*(I-1)*dT)
     +             +Z2)/1000.00-Z10*CMD21(I,2)/1000)

        CMD21(I+1,1)=CMD21(I,1)+dT/((Z4*((I-1)*dT)**3+
     +                          Z3*((I-1)*dT)**2+
     +                          Z2*(I-1)*dT+Z1)/1000)*
     +             (X(6)*CMD21(I,2)*EXP(-X(8)*(I-1)*dT)
     +             -CMD21(I,1)*((3*Z4*((I-1)*dT)**2+2*Z3*(I-1)*dT)
     +             +Z2)/1000.00-Z10*CMD21(I,1)/1000)
40      continue


        open (unit=2,file='exp16.dat',status='old')
        read (2,*)((C16(i,j),j=1,4),i=1,21)
        close (unit=2)

        CMD16(1,4)=C16(1,4)
        CMD16(1,3)=0.0
```

```
      CMD16(1,2)=0.0
      CMD16(1,1)=0.0

      do 10 I=1,300

      CMD16(I+1,4)=CMD16(I,4)+dT/((V4*((I-1)*dT)**3+
     +                            V3*((I-1)*dT)**2+
     +                            V2*(I-1)*dT+V1)/1000)*
     +             (-(X(3)+X(4))*CMD16(I,4)*EXP(-X(8)*(I-1)*dT)
     +             -CMD16(I,4)*((3*V4*((I-1)*dT)**2+2*V3*(I-1)*dT)
     +             +V2)/1000.00-V10*CMD16(I,4)/1000)
      CMD16(I+1,3)=CMD16(I,3)+dT/((V4*((I-1)*dT)**3+
     +                            V3*((I-1)*dT)**2+
     +                            V2*(I-1)*dT+V1)/1000)*
     +             (X(3)*CMD16(I,4)*EXP(-X(8)*(I-1)*dT)
     +             -X(6)*CMD16(I,3)*EXP(-X(8)*(I-1)*dT)-CMD16(I,3)
     +             *((3*V4*((I-1)*dT)**2+2*V3*(I-1)*dT)+V2)/1000.00
     +              -V10*CMD16(I,3)/1000)
      CMD16(I+1,2)=CMD16(I,2)+dT/((V4*((I-1)*dT)**3+
     +                            V3*((I-1)*dT)**2+
     +                            V2*(I-1)*dT+V1)/1000)*
     +             (X(4)*CMD16(I,4)*EXP(-X(8)*(I-1)*dT)
     +             -X(7)*CMD16(I,2)*EXP(-X(8)*(I-1)*dT)-CMD16(I,2)
     +             *((3*V4*((I-1)*dT)**2+2*V3*(I-1)*dT)+V2)/1000.00
     +             -V10*CMD16(I,2)/1000)
      CMD16(I+1,1)=CMD16(I,1)+dT/((V4*((I-1)*dT)**3+
     +                            V3*((I-1)*dT)**2+
     +                            V2*(I-1)*dT+V1)/1000)*
     +             (X(6)*CMD16(I,3)*EXP(-X(8)*(I-1)*dT)
     +             +X(7)*CMD16(I,2)*EXP(-X(8)*(I-1)*dT)-CMD16(I,1)
     +             *((3*V4*((I-1)*dT)**2+2*V3*(I-1)*dT)+V2)/1000.00
     +              -V10*CMD16(I,1)/1000)

10    CONTINUE
```

```
      open (unit=3,file='exp17.dat',status='old')
      read (3,*)((C17(i,j),j=1,3),i=1,21)
      close (unit=3)


      CMD17(1,3)=C17(1,3)
      CMD17(1,2)=0.0
      CMD17(1,1)=0.0

      do 20 I=1,300

      CMD17(I+1,3)=CMD17(I,3)+dT/((U4*((I-1)*dT)**3+
     +                          U3*((I-1)*dT)**2+
     +                          U2*(I-1)*dT+U1)/1000)*
     +            (-X(5)*CMD17(I,3)*EXP(-X(8)*(I-1)*dT)-CMD17(I,3)
     +            *((3*U4*((I-1)*dT)**2+2*U3*(I-1)*dT)+U2)/1000.00
     +             -U10*CMD17(I,3)/1000)

      CMD17(I+1,2)=CMD17(I,2)+dT/((U4*((I-1)*dT)**3+
     +                          U3*((I-1)*dT)**2+
     +                          U2*(I-1)*dT+U1)/1000)*
     +            (X(5)*CMD17(I,3)*EXP(-X(8)*(I-1)*dT)-
     +            X(7)*CMD17(I,2)*EXP(-X(8)*(I-1)*dT)-CMD17(I,2)
     +            *((3*U4*((I-1)*dT)**2+2*U3*(I-1)*dT)+U2)/1000.00
     +            -U10*CMD17(I,2)/1000)
      CMD17(I+1,1)=CMD17(I,1)+dT/((U4*((I-1)*dT)**3+
     +                          U3*((I-1)*dT)**2+
     +                          U2*(I-1)*dT+U1)/1000)*
     +            (X(7)*CMD17(I,2)*EXP(-X(8)*(I-1)*dT)-CMD17(I,1)
     +            *((3*U4*((I-1)*dT)**2+2*U3*(I-1)*dT)+U2)/1000.0
     +            -U10*CMD17(I,1)/1000)

20    CONTINUE
```

```
      open (unit=4,file='exp15.dat',status='old')
      read (4,*)((C15(i,j),j=1,6),i=1,21)
      close (unit=4)

      CMD15(1,6)=C15(1,6)
      CMD15(1,5)=0.0
      CMD15(1,4)=0.0
      CMD15(1,3)=0.0
      CMD15(1,2)=0.0
      CMD15(1,1)=0.0


      do 30 I=1,300


      CMD15(I+1,6)=CMD15(I,6)+dT/((Y4*((I-1)*dT)**3+
     +                            Y3*((I-1)*dT)**2+
     +                            Y2*(I-1)*dT+Y1)/1000)*
     +          (-(X(1)+X(2))*CMD15(I,6)*EXP(-X(8)*(I-1)*dT)-
CMD15(I,6)
     +             *((3*Y4*((I-1)*dT)**2+2*Y3*(I-1)*dT)+Y2)/1000.00
     +           -Y10*CMD15(I,6)/1000)
      CMD15(I+1,5)=CMD15(I,5)+dT/((Y4*((I-1)*dT)**3+
     +                            Y3*((I-1)*dT)**2+
     +                            Y2*(I-1)*dT+Y1)/1000)*
     +             (X(1)*CMD15(I,6)*EXP(-X(8)*(I-1)*dT)
     +          -(X(3)+X(4))*CMD15(I,5)*EXP(-X(8)*(I-1)*dT)-CMD15(I,5)
     +             *((3*Y4*((I-1)*dT)**2+2*Y3*(I-1)*dT)+Y2)/1000.00
     +            -Y10*CMD15(I,5)/1000)
      CMD15(I+1,4)=CMD15(I,4)+dT/((Y4*((I-1)*dT)**3+
     +                            Y3*((I-1)*dT)**2+
     +                            Y2*(I-1)*dT+Y1)/1000)*
     +             (X(2)*CMD15(I,6)*EXP(-X(8)*(I-1)*dT)
     +             -X(5)*CMD15(I,4)*EXP(-X(8)*(I-1)*dT)-CMD15(I,4)*
     +             ((3*Y4*((I-1)*dT)**2+2*Y3*(I-1)*dT)+Y2)/1000.00
```

```
     +              -Y10*CMD15(I,4)/1000)
       CMD15(I+1,3)=CMD15(I,3)+dT/((Y4*((I-1)*dT)**3+
     +                          Y3*((I-1)*dT)**2+
     +                          Y2*(I-1)*dT+Y1)/1000)*
     +            (X(3)*CMD15(I,5)*EXP(-X(8)*(I-1)*dT)
     +            -X(6)*CMD15(I,3)*EXP(-X(8)*(I-1)*dT)-CMD15(I,3)
     +            *((3*Y4*((I-1)*dT)**2+2*Y3*(I-1)*dT)+Y2)/1000.00
     +             -Y10*CMD15(I,3)/1000)
       CMD15(I+1,2)=CMD15(I,2)+dT/((Y4*((I-1)*dT)**3+
     +                          Y3*((I-1)*dT)**2+
     +                          Y2*(I-1)*dT+Y1)/1000)*
     +            (X(4)*CMD15(I,5)*EXP(-X(8)*(I-1)*dT)
     +            -X(5)*CMD15(I,4)*EXP(-X(8)*(I-1)*dT)
     +            -X(7)*CMD15(I,2)*EXP(-X(8)*(I-1)*dT)-CMD15(I,2)*
     +            ((3*Y4*((I-1)*dT)**2+2*Y3*(I-1)*dT)+Y2)/1000.00
     +             -Y10*CMD15(I,2)/1000)
       CMD15(I+1,1)=CMD15(I,1)+dT/((Y4*((I-1)*dT)**3+
     +                          Y3*((I-1)*dT)**2+
     +                          Y2*(I-1)*dT+Y1)/1000)*
     +            (X(6)*CMD15(I,3)*EXP(-X(8)*(I-1)*dT)
     +            +X(7)*CMD15(I,2)*EXP(-X(8)*(I-1)*dT)-CMD15(I,1)
     +            *((3*Y4*((I-1)*dT)**2+2*Y3*(I-1)*dT)+Y2)/1000.0
     +            -Y10*CMD15(I,1)/1000)


30     CONTINUE



       w1=1.0
       w2=1.0
       w3=1.0
       w4=1.0
       w5=1.0
       w6=1.0
```

```
      w7=1.0
      w8=1.0
      w9=1.0
      w10=10.0
      w11=1.0
      w12=1.0
      w13=1.0
      w14=1.0
      w15=1.0

      SUM=0.0
      DO 50 K=1,16

      E=w1*(CMD16((K-1)*20+1,4)-C16(K,4))**2+
     +   w2*(CMD16((K-1)*20+1,3)-C16(K,3))**2+
     +   w3*(CMD16((K-1)*20+1,2)-C16(K,2))**2+
     +   w4*(CMD16((K-1)*20+1,1)-C16(K,1))**2+
     +   w5*(CMD17((K-1)*20+1,1)-C17(K,1))**2+
     +   w6*(CMD17((K-1)*20+1,2)-C17(K,2))**2+
     +   w7*(CMD17((K-1)*20+1,3)-C17(K,3))**2+
     +   w8*(CMD15((K-1)*20+1,6)-C15(K,6))**2+
     +   w9*(CMD15((K-1)*20+1,5)-C15(K,5))**2+
     +   w10*(CMD15((K-1)*20+1,4)-C15(K,4))**2+
     +   w11*(CMD15((K-1)*20+1,3)-C15(K,3))**2+
     +   w12*(CMD15((K-1)*20+1,2)-C15(K,2))**2+
     +   w13*(CMD15((K-1)*20+1,1)-C15(K,1))**2+
     +   w14*(CMD21((K-1)*20+1,2)-C21(K,2))**2+
     +   w15*(CMD21((K-1)*20+1,1)-C21(K,1))**2


      SUM=SUM+E
50    CONTINUE


      F=SUM
```

```
      print*, F
      print*,'k1=',X(1),'  k2=',X(2),'  k3=',X(3),'  k4=',X(4)
      print*,'k5=',X(5),'  k6=',X(6),'  k7=',X(7),'  kd=',X(8)


      return
      END


C     ======================================================
      SUBROUTINE DATA(TIME,V1,V2,V3,V4,V5,V6,V7,V8,V9,V10,
     +                U1,U2,U3,U4,U5,U6,U7,U8,U9,U10,
     +                Y1,Y2,Y3,Y4,Y5,Y6,Y7,Y8,Y9,Y10,
     +                Z1,Z2,Z3,Z4,Z5,Z6,Z7,Z8,Z9,Z10)
      real TIME,V1,V2,V3,V4,V5,V6,V7,V8,V9,V10,
     +       U1,U2,U3,U4,U5,U6,U7,U8,U9,U10,
     +       Y1,Y2,Y3,Y4,Y5,Y6,Y7,Y8,Y9,Y10,
     +       Z1,Z2,Z3,Z4,Z5,Z6,Z7,Z8,Z9,Z10

      DIMENSION TIME(21)


      TIME(1)=0.00
      TIME(2)=1.00
      TIME(3)=2.00
      TIME(4)=3.00
      TIME(5)=4.00
      TIME(6)=5.00
      TIME(7)=6.00
      TIME(8)=7.00
      TIME(9)=8.00
      TIME(10)=9.00
      TIME(11)=10.00
      TIME(12)=11.00
```

```
TIME(13)=12.00
TIME(14)=13.00
TIME(15)=14.00
TIME(16)=15.00
TIME(17)=20.00
TIME(18)=25.00
TIME(19)=30.00
TIME(20)=40.00
TIME(21)=60.00

U1=200.0
U2=0.1821
U3=-0.0657
U4=0.0022
U5=193.6
U6=0.0708
U7=0.0037
U8=0.2488
U9=-0.0021
U10=0.8

V1=200.00
V2=-0.0391
V3=-0.0391
V4=0.0013
V5=192.24
V6=0.1337
V7=0.0033
V8=0.2488
V9=-0.0021
V10=0.8

Y1=200.0
Y2=-0.6229
Y3=0.0194
```

```
Y4=-0.0008
Y5=191.64
Y6=-0.0012
Y7=0.0027
Y8=0.2378
Y9=-0.0015
Y10=0.8

Z1=200.0
Z2=2.2439
Z3=-0.2629
Z4=0.0087
Z5=200.0
Z6=0.2162
Z7=0.003
Z8=0.2488
Z9=-0.0021
Z10=0.8

return
end
```

APPENDIX G

FORTRAN PROGRAM FOR SOLVING DECHLORINATION OF 2,4,6-TRICHLOROPHENOL ON ALGINATE BEAD ENTRAPPED Pd/Fe CATALYST MODEL

```
C  exp29.for
c
c  exp29 data
c  dechlorination of 2,4,6-TCP in fluidized bed without applying
c  field
c
c  kl:X(3) mass transfer coeff.
c  De:X(4) diffusion coeff.
c  k: X(1) reaction rate constant
c  kd:X(2) deactivation constant
C
C                          DECLARATION OF VARIABLES

      INTEGER N,M,J
      PARAMETER (N=4)
C
      INTEGER I, MAXFN, NOUT
      REAL  DFPRED, FVALUE, G(N), GRADTL, X(N),XGUESS(N), XS(N)
      real C23(9),CMD23(121,12),TIME(9),Kb
      common CMD23
      EXTERNAL ROSBRK, UMACH, UMCGF
C
      DATA XGUESS/0.009,0.01,0.0004,0.01/,
     +  XS/4*1.0E0/
C
      DFPRED = 0.000000001
      GRADTL = 1.E-12
      MAXFN = 0
```

```
C                              MINIMIZE THE ROSBRK FUNCTION

      CALL UMCGF (ROSBRK, N, XGUESS, XS, GRADTL,MAXFN, DFPRED,
     + X, G, FVALUE)

C                              PRINT THE VALUE


      CALL UMACH (2, NOUT)
      WRITE (NOUT,99999) (X(I), I=1, N), FVALUE, (G(I),I=1,N)
99999  FORMAT ('SOL:', 4(1x,E10.3), //,'THE FUNCTION '
     + 'EVALUATED AT THE SOLUTION IS ',2X,E10.3,//,
     + 'GRAD:',4(1x,E9.3),/)
C

      CALL DATA(TIME,VL,Vb,Ep,Kb,r0)

      open(unit=5,file='29ksd.dat',status='new')
      do 150 K=1,9
      write(5,99)(CMD23((K-1)*15+1,12))
99    format(2x,E10.3)
150   continue
      close(unit=5)

      END
C     ============================================================
      SUBROUTINE ROSBRK (N, X, F)
      INTEGER N
      REAL X(N), F


      INTEGER i,j,h
      REAL C23(9),CMD23(121,12),dt,dr,Kb
      common CMD23
```

```
      CALL DATA(TIME,VL,Vb,Ep,Kb,r0)

      dt=2.0
      dr=0.01

      open (unit=2,file='exp29.dat',status='old')
      read (2,*)(C23(i),i=1,9)
      close (unit=2)



      CMD23(1,12)=C23(1)
      CMD23(1,11)=C23(1)


      do 10 i=1,10
      CMD23(1,i)=0.0
10    continue

      do 20 j=2,121
      CMD23(j,12)=CMD23(j-1,12)-dt*((1.0-Ep)/Ep)*(3.0/r0)*X(3)*100*
     + (CMD23(j-1,12)-CMD23(j-1,11)/Kb)

      do 30 h=10,2,-1
      CMD23(j,h)=CMD23(j-1,h)+dt*(2.0/((h-1)*dr)*X(4)/1000*
     +          (CMD23(j-1,h+1)-CMD23(j-1,h))/dr+
     +          X(4)/1000*(CMD23(j-1,h+1)-2.0*CMD23(j-1,h)+
     + CMD23(j-1,h-1))/(dr**2)-X(1)*10000/Vb/(1-0.186)*
     + (CMD23(j-1,h+1)
     +  +CMD23(j-1,h))
     + /2.0*exp(-X(2)*(j-1)*dt))
30    continue

      CMD23(j,1)=CMD23(j,2)
```

```
      CMD23(j,11)=(1/(1/dr+X(3)*100/(X(4)/1000*(1-0.186))))*
     +            (X(3)*100/(X(4)/1000*(1-0.186))*CMD23(j,12)+
     +             CMD23(j,10)/dr)


20    continue

      SUM=0.0
      do 50 i=1,9
      F=(CMD23((i-1)*15+1,12)-C23(i))**2
      SUM=SUM+F
50    continue
      F=SUM



      print*, F
      print*,'kl=',X(3),'    De=',X(4)
      print*,'k=',X(1),'    kd=',X(2)

      return
      END


C     ======================================================
      SUBROUTINE DATA(TIME,VL,Vb,Ep,Kb,r0)
      real TIME,VL,Vb,Ep,Kb,r0
      DIMENSION TIME(9)

      TIME(1)=0.00
      TIME(2)=30.00
      TIME(3)=60.00
      TIME(4)=90.00
```

```
TIME(5)=120.00
TIME(6)=150.00
TIME(7)=180.00
TIME(8)=210.00
TIME(9)=240.00


VL=2100.0
Vb=110.0
Ep=VL/(VL+Vb)
Kb=1.0
r0=0.1

return
end
```

APPENDIX H

Calculation of the Diffusivity of 2,4,6-trichlorophenol Into Water

Wilke-Chang (1955) equation is used for calculatio the diffusion coefficient of 2,4,6-trichlorophenol in water. The equation is:

$$D_{AB} = \frac{T}{\mu_B} \frac{7.4x10^{-8}\sqrt{\Phi_B M_B}}{V_A^{0.6}} \qquad \text{(H.1)}$$

where,

Φ_B is the association factor for water : 2.26

M_B is the molecular weight of water: 18 [g/mol]

T= 293[K]

μ_B is the viscosity of water: 0.993 [cp]

V_A is the molar volume of 2,4,6-trichlorophenol: 157.1 [cm^3/mol]

Substituting above values into Equation H.1 yields:

$D_{AB}=6.7x10^{-10}$[m^2/s]